Advances in forward osmosis membranes: Altering the sub-layer structure via recent fabrication and chemical modification approaches

*Wafa Ali Suwaileh[1], Daniel James Johnson[1], Sarper Sarp[1], Nidal Hilal[1,2]**

[1]Centre for Water Advanced Technologies and Environmental Research (CWATER), College of Engineering, Swansea University, Fabian Way, Swansea SA1 8EN, UK.

[2] College of Engineering, University of Sharjah, P.O.Box 27272 Sharjah, United Arab Emirates

*Corresponding author: n.hilal@swansea.ac.uk

Abstract

The forward osmosis process has obtained renewed interest nowadays and it might become an alternative solution for many industrial applications to meet the current and future requirements for potable water. The FO process depends on the osmotic pressure gradient between a high salinity draw solute and low salinity feed solution across a semi-permeable membrane to extract pure water. Despite the potential advantages of FO, there are some technical drawbacks that hinder FO application for water desalination. One of the most significant critical challenges is the need for membrane compatible with the FO process. To improve FO desalination feasibility, membrane development is required to obtain maximum water permeability and minimum

reverse solute flux over long-term operations. Therefore, this review starts by demonstrating the fundamentals and membrane development over the years. Fabrication modifications for the support layer of FO membranes and the crucial challenges of the FO process are summarized. Recent trends of the chemical modifications of the bulk and substrate are discussed. The advantages and disadvantages of the modifications on the FO membrane productivity are also addressed. Finally, concluding with future perspectives.

Highlights

- Comprehensive overview of commercial FO membranes and modified FO sub-layers.
- Discussion of fundamental and practical challenges of FO membrane performance.
- Chemical modification strategies to minimize the structural parameter of FO sub-layer.
- Research prospects for further promoting FO membrane productivity.

Keywords

Forward osmosis, desalination, chemical modifications, membrane fabrication, support layer, synthetic polymer, nanotechnology.

List of contents

List of abbreviations

FO	Forward osmosis
RO	Reverse osmosis
TFC	Thin film composite
PA	Polyamide
CA	Cellulose acetate
CTA	Cellulose triacetate
MMM	Mixed matrix membranes
PSf	Polysulfone
AqpZ	Aquaporin
NIPS	Non-solvent induced phase separation
L-b-L	Layer by layer technique
MPD	2-methyl-2,4-pentanediol
TMC	1, 3, 5-trimesoylchloride
FS	Feed solution
DS	Draw solution
ICP	Internal concentration polarization
ECP	External concentration polarization
PES	Polyether sulfone
pNE	Norepinephrine

HTI	Hydration Technology Innovations
SDS	Sodium dodecyl sulfate
Zn_2GeO_4	Nanowires
IER-Na	Na type ion exchange resin
PEM	Polyelectrolyte multilayer
SA	Sodium alginate
LiCl	Lithium chloride
PI	Phase inversion technique
PEG	Polyethylene glycol-electrolyte
PRO	Pressure retarded osmosis
NaCl	Sodium chloride
PBI	Polybenzimidazole
NF	Nanofiltration
IP	Interfacial polymerization
PBI-PES	Polybenzimidazole-polyethersulfone
CNTs	Carbon nanotubes
PAI	Poly(amide–imide)
PET	Polyethylene terephthalate
PAN	Polyacrylonitrile
ZnO-SiO_2	Zinc oxide-Silicon dioxide
TiO_2-g-PHEMA	Titanium dioxide grafted poly(2-hydroxyethyl methacrylate)
MWCNTs	Multiwalled carbon nanotubes
f-CNTs	Functionalized multi-walled carbon nanotubes
PVDF	Polyvinylidene fluoride
SiO_2	Silicon dioxide
TiO_2	Titanium dioxide
PVA	Polyvinyl alcohol

MA	Maleic acid
PAA	Polyacrylic acid
CP	Concentration polarization
CEOP	Cake-enhanced osmotic pressure
sPPSU	Sulfonated poly phenylene sulfone
sPSf	Sulfonated polysulfone
sPES	Sulfonated polyether sulfone
NPs	Nanoparticles
SO_3H	Sulfonic acid groups
MMT	Montmorillonite
PESU E6020P	Polyethersulfone
PPSU	Polyphenyl sulfone
CPSF	Carboxylated polysulfone
CPES	Carboxylic polyethersulfone
PTA–POD	Polytriazole-co-polyoxadiazole
SPEK	Sulphonated poly(ether ketone)
PFSA	Perfluorosulfonic acid
NMP	N-Methyl-2-pyrrolidone
GO	Graphene oxide
CN/rGO	Graphene oxide based graphitic carbon nitride
HNTs	Alumina-Silicates
MWf	Functionalized Multiwalled Carbone Nanotubes
GOT or MWfT	Carbon-TiO_2 composite
PVP	Polyvinyl pyrrolidone
PAH	Polyallylamine hydrochloride
$CaCO_3$	Calcium Carbonate
HCl	Hydrochloric acid

LDH-NPs	layered double hydroxide nanoparticles
PDA	Phenylenediamine
SW	Seawater
BW	Brackish water
GA	Glutaraldehyde
CMBA	4-(chloromethyl) benzoic acid
EDC	N-ethyl-N(3-dimethylamino) carbodiimide
$MgSO_4$	Magnesium sulphate
Na_2SO_4	Sodium Sulphate
$MgCl_2$	Magnesium Chloride
PEI	Polyethyleneimine
NaOH	Sodium hydroxide
PEI	Polycationethyleneimine
PSS	Polyanion polystyrene sulfonate
H-PAN	Hydrolyzed polyacrylonitrile
DOPC	1,2-dioleloyl-sn-glycero-3-phosphocholine
DOTAP	1,2-dioleoyl-3-trimethylammo-nium-propane (chloride salt)
T-PSS	PSS-terminated double-skinned
SLB	Supported lipid bilayer
SO_3	Sulfonic group

List of symbols

$\Delta\pi$	Osmotic pressure gradient
π	Osmotic pressure
V	Solution volume

R	Ideal gas constant
8.314 J K^{-1} mol^{-1}	Ideal gas constant unit
T	Absolute temperature in Kelvin
B2, B3, B4	Viriel empirical coefficients
σ	Reflection coefficient
π_D	Bulk osmotic pressures of the draw solute
π_F	Bulk osmotic pressures of the feed solution
B	Salt permeability coefficient
A	Water permeability coefficient
E	Global error
EXP	Experimental flux
CALC	Calculated flux
k/k_F	Mass transport coefficient of the feed solution/solute resistance
D	Bulk diffusion coefficient of the draw solute
SS_{err}	Residual sum of squares
SS_{TOT}	Total sum of squares
R^2_s	Coefficient of determination for the solute flux
τ	Membrane support layer tortuosity
t_s	Thickness
A/B	Selectivity ratio of membrane active layer: water permeability/salt permeability
S	Membrane support layer structure parameter
ε_{eff}	Effective porosity
PH	Potential of hydrogen
$D\epsilon_{eff}$	Effective diffusion constant
M	Molar concentration
LMH	Water flux unit

wt %	Mass fraction or weight percent of nanoparticles
g L^{-1}	Grams per liter: specific reverse solute flux unit
mm, µm	Support layer thickness unit
J_s	Salt leakage or salt reverse flux
$gm^{-2}h^{-1}$, gMH, $mol/m^{-2}h^{-1}$	Salt leakage or salt reverse flux unit
J_w	Water flux
J_s/J_w	Ratio of salt flux to water flux
mol%	Mole percent: a percentage of the moles of a specific constituent are of the total moles which are in a mixture.
^oC	Degree Celsius
Mol/ l	Molar concentration unit
(J_w/J_s)	The ratio of reverse solute flux selectivity
Nm, µm	Membrane active layer thickness
nm	Nanometer: the nanoparticle size and mean pore size of the active layer
KPa	Kilopascal: Membrane active layer selectivity unit
mM	Millimolar concentration
ppm	Parts per million concentration
h	Hour for reaction time
Mol/L	Moles per litre or molarity concentration
mg/L	Milligrams per litre concentration
wt./v %	Weight/volume percent: mass concentration of zeolite
Vol%	Volume fraction

1 Introduction

The growth of the global population and the rise in water consumption has increased the already great pressure on water and energy systems [1]. Two alternatives for increasing water supplies involve desalination of sea or brackish water or the reclamation of wastewater [2]. A promising emerging membrane technology for purification of water is forward osmosis process which has gained immense interest since the mid-1970s [3]. Osmosis is a natural process which involves the transfer of water molecules throughout a porous membrane [4]. In order to induce the flow of water from one to another side, an osmotic pressure differential is required. The FO system operates using a permeable membrane and two solutions with different concentrations, the feed solution (FS) and draw solution (DS). The osmotic pressure gradient between low concentration FS (low osmotic pressure) and high concentration DS (high osmotic pressure) is the driving force. Accordingly, the difference in osmotic pressure drives the water through a semi-permeable membrane to the higher osmotic pressure side while hindering the transport of ions [5, 6, 7, 8]. In a typical FO system, the selective layer is in contact with the feed solution and the support layer is in contact with draw solute. FO operates without the need of applied hydraulic pressure, leading to reduced irreversible fouling tendency [5]. It is highly efficient for various contaminants, has low energy consumption and potentially achieves high recovery [9], although this does not include any additional contributions or costs if draw solute regeneration is needed. Therefore, FO can be of strategic importance in food and pharmaceutical manufacturing, treating landfill leachate, treatment of highly saline streams, seawater and industrial wastewater purification[4, 5, 10, 11, 12].

Considerations, such as low water quality in a single stage [3], draw solution properties, reverse salt flux [5] and the choice of an ideal FO membrane are critical for the development of the FO desalination system [11]. A wide range of membranes have been used for the FO process in both flat sheet and hollow fibre configurations including cellulose acetate (CA), cellulose triacetate

(CTA), thin film composite (TFC), and bio-mimetic membranes [13]. Amongst FO membranes, the cellulosic membrane has been employed widely for the FO process; however, it suffers low selectivity, is prone to biological attack and chemical hydrolysis [14]. Thereafter, desalination researchers focused on unique TFC-FO membranes for the FO system because of excellent water permeability and selectivity arising from a porous sub-layer and a thin active layer [15]. The design of the TFC asymmetric membrane is shown in Fig.1. It has a thin support layer embedded with a mesh for mechanical strength. A thin active layer was formed on the top of the support layer [16]. Subsequently, mixed matrix membranes (MMM) have been used for the FO process. They consist of the deposition of filler into the polymer matrix presenting a good surface area, water permeation and separation properties [17]. This new domain was considered for two reasons: firstly, the hydrophobic nature of the most membrane polymers and secondly, a hydrophilic sub-layer can be affected by water and got plasticized while the selective layer was more rigid [18]. A new attractive protein material is Aquaporin which has been incorporated into either a substrate or selective layer to form a flat sheet or hollow fibre membranes [13, 19].The FO membranes can be fabricated via phase inversion methods that can be further classified into thermally induced phase separation, precipitation by controlled evaporation, vapour phase precipitation, and non-solvent induced phase separation (NIPS) [20].

Phase inversion is the most important and successful technique used for the preparation of flat sheet and hollow fibre FO membranes. It involves mixing a polymer with solvent and casting of the polymer suspension on a support layer. The next step is the immersion precipitation of this support layer which could be described as soaking a polymer solution in a non-solvent coagulant bath [21]. In addition to this process, a dry-jet wet spinning process was also used to fabricate a hollow fibre substrate [22]. It consists of preparing a polymer dope which was extruded by a spinneret at a volume rate that was fixed by a gear pump. Subsequently, it was subjected to an

air gap followed by a soaking in a coagulation bath. Electro-spinning is another technique used for the formation of fibrous polymer in various configurations and functions. It has been employed to fabricate flat sheet and hollow fibre membranes. It involves applying a high electrical field to a polymer suspension in a syringe. This will result in ejecting and depositing fine fibres on a collector [23, 24, 25, 26]. The layer by layer technique (L-b-L) is used to synthesize FO membranes which involve exposing the prefabricated sub-layer to a polyelectrolyte with an opposite charge for a limited time. This creates a uniform and homogenous ultra-thin selective film on the surface [27, 28]. By adding alternately charged polyelectrolytes, multi-layers can be formed. The selective layer was synthesized byinterfacial polymerization that is based on the interaction between m-phenylenediamine (MPD) and trimesoyl chloride (TMC) monomers to form a very thin film [29]. This membrane had an asymmetric structure and high permeability and was used for FO processes. The major objective is to synthesize a FO membrane having excellent water permeability, the good rejection rate for salt and foulants, and stable water flux during long-term operations. Nevertheless, the practicality of the sub-layer design is restricted due to some serious problems. For example, the thickness of the porous sub-layer is of crucial importance on the water flux due to an increment of mass transfer resistance and the effects of internal concentration polarization (ICP). The ICP occurs due to the dilution of the concentrated draw solute across the sub-layer while the precipitation of the feed molecules is across the selective layer, causing a decrease in the water flux of up to >80% [9, 30]. In order to alleviate the ICP, optimizing the sub-layer structure such as thickness, tortuosity, and porosity via the fabrication methods is essential. Up to date, extensive research efforts have been conducted to manufacture an appropriate support layer for the FO membrane through adjusting the phase inversion procedure. For example, a sub-layer of CTA membrane was modified via different conditions of phase inversion. The solvent and non-solvent were replaced by a mixture of dioxane and acetone and a mixture of

lactate and methanol respectively. The concentration of the polymer and additives were also varied [31]. Replacing the solvent and non-solvent and changing the concentration on both the polymer and additives resulted in a very open sub-layer. Thus, the water flux enhanced but low salt rejection is still a critical problem. Another attempt proposed modifying the polysulfone (PSf) sub-layer structure of a flat sheet TFC-FO membrane by phase inversion method. It was speculated that the thickness and chemistry of the sub-layer may influence the solute mass transfer resistance [11]. Hence, when the PSf sub-layer was made of a dense sponge-like structure, the mass transport was hindered, leading to lower water permeation [32]. The performance of FO membranes could be affected by ICP arising from the spongy and tortuous structure [33]. In addition, there are several chemical procedures for polymeric membranes such as physical, surface chemical treatments and chemical modification of the base polymer [34, 35]. The most common procedures studied for FO membranes are the chemical modification of the base polymer and the substrate. Here, the chemical treatment was accomplished by depositing chemical agents using different methods to improve the membrane performance [36]. Chemical modification can be achieved during synthesis by embedding hydrophilic additives or nanomaterials into the polymer matrix. There are two important elements to develop ideal TFC-FO membrane, which involves good wetting and hydrophilicity of the sub-layer. Therefore, the former will facilitate the diffusion of the solution in wetted pores while the latter will help in reducing the ICP impact [37].Some other potential methods are the deposition of inorganic nanoparticles and metal oxide nanoparticles into the sub-layer of the FO membrane [38, 39]. When nanosilica particles were incorporated into the polysulfone substrate, more pathways for water transfer were created in the porous sub-layer [40]. This was attributed to an increase in the hydrophilicity aiding to enhanced water flux. However, high content of nanoparticles caused a defect in the active layer, arising from an aggregation of the nanoparticles. This possessed lower

water flux and higher salt permeability. This can increase the ICP effects, resulting in reducing the water transport through the membrane. Other recent work describes improving the substrate hydrophilicity by Norepinephrine (pNE) coating on a double-structured sub-layer [41]. A moderate enhancement in water flux was observable. However, it has some drawbacks; for example, it is expensive and should be prepared with the addition of oxidant under corrosive preparation conditions.

In light of this, there is very little work that addresses the progress of the fabrication and chemical modifications of the FO sub-layer to improve the membrane performance. Thus, this review paper will first demonstrate the physical concept and performance evaluation of the FO process. It will give an overview of work which has been undertaken so far on the fabrication and chemical modifications in the synthetic polymer and on the substrate, including comparison between these approaches in terms of membrane performance. Lastly, it will discuss the advantages and disadvantages of the chemical modifications on different FO support layers where relevant.

2 Theoretical background of FO process

2.1 The principle

In accordance with the second law of thermodynamics, the FO process depends on the chemical potential difference between low salinity feed and high salinity draw solute [42, 43]. Then the water flows from low salinity solution through a semi-permeable membrane to the high salinity solution, leading to equilibrium of the chemical potential. Practically, the role of a high salinity DS (e.g. sodium chloride, NaCl) is to produce the osmotic pressure gradient ($\Delta\pi$) needed to draw water from low salinity feed (e.g. seawater) within a permeable membrane to the permeate side (concentrated solution) while reverse salt flux is unavoidable as described in Fig.2 [44]. The

separation of the feed solutions and solutes occur in the low salinity stream because of osmotic pressure gradients and the membrane properties. As a result, the feed solution becomes concentrated while the high salinity draw solute becomes diluted. At this stage, the osmotic pressure gradient decreases, arising from the change in the solution's concentrations. The water transport is discontinued when the driving force of the process diminishes due to equilibrium between the osmotic pressure gradient and the opposing hydrostatic pressure [45].

This osmotic pressure (π) is influenced by the draw solute concentration and its temperature [46]. Accordingly, the osmotic pressure of a diluted solution, containing dissociated electrolyte of Np ions, can be determined using the Van't Hoff equation [47]:

$$\pi = \frac{N_p RT}{V} = MRT \tag{47}$$

In which, π, V are the osmotic pressure and the solution volume respectively, M is the molar concentration (mol l^{-1}) while R is the ideal gas constant (8.314 J K^{-1} mol^{-1}) and T is the absolute temperature in Kelvin. It should be noted that this equation is invalid for a concentrated solution used in the FO system. Therefore, the osmotic pressure of this solution can be estimated by the virial expansion [48]:

$$\pi = cRT\left(\frac{1}{M} + B_2 c + B_3 c^2 + B_4 c^3 \ldots\right) \tag{48}$$

Where c refers to the mass concentration of the solute while B2, B3, B4 etc are empirical virial coefficients. It can be estimated by an osmometer, freezing point depression osmometer and the solution vapour pressure [47]. Because the FO process uses the osmotic pressure gradient, it does not require applied hydraulic pressure. Ideally, the performance of a fabricated FO membrane

and its characteristics can be assessed by quantifying the pure water and reverse solute fluxes [49] which will be addressed below.

2.2 Determination of membrane transport parameters

The FO sub-layer design has an important role in controlling the diffusion of the draw solute which contributes to effective FO membrane performance. Fig.3 demonstrates the special requirements to make FO membrane feasible, including the selection of the material and the morphology. Also, there are a number of factors that should be considered, such as water permeation, selectivity, strength, stability and ICP effect to achieve the best FO membrane performance.

Experimentally, the pure water permeability coefficient (A), the solute permeability coefficient (B) and the structural parameter (S) describe the intrinsic properties of an FO membrane performance. The A and B values can be estimated from the RO test while the S value can be quantified by measuring the initial water flux in the FO test. Phuntsho et al [50] expressed the water flux and included the reflection coefficient (σ) as follows:

$$J_w = A\,\sigma\,[\pi_D - \pi_F] \tag{50}$$

Where A denotes the pure water permeability, σ is the reflection coefficient while π_D and π_F refer to the bulk osmotic pressures of the DS and the FS respectively. However, σ is approximately 1 when the membrane has high NaCl rejection (>93-95%) and therefore, it can be neglected. A low σ value means low effect of osmotic force arising from the salt reverse flux [4]. Importantly, the B value depends on the solute diffusion coefficient. It should be reduced to minimize the salt reverse flux. This is because salt reverse flux causes a low osmotic pressure due to a reduction in π_F and an increase in π_D. In contrast, a thin FO membrane possibly deforms or cracks under hydraulic pressure during the RO test. This is because the FO membrane has poor mechanical

strength to tolerate a significant hydraulic pressure. Therefore, the RO test may provide an unreliable assessment of the FO membrane performance and affects the accuracy of the RO-FO hybrid system [51]. Instead, Tiraferri et al [52] proposed an algorithm based on the water and salt flux results to quantify the A, B, and S. The procedure consists of four steps involving a non-dimensional sum of the offsets in the water and salt fluxes described by the global error, E, is given by:

$$E = E_w + E_s = \sum_{i=1}^{n} \left(\frac{J_{w,i}^{EXP} - J_{w,i}^{CALC}}{J_w^{-EXP}, n} \right)^2 + \sum_{i=1}^{n} \left(\frac{J_{s,i}^{EXP} - J_{s,i}^{CALC}}{J_s^{-EXP}, n} \right)^2 \quad (52)$$

Where, n = 4 describe the number of the steps, while the superscripts EXP and CALC are the experimental and calculated fluxes from the following equations:

$$J_w = A \left\{ \frac{\pi_D exp\left(-\frac{J_w S}{D}\right) - \pi_F exp\left(\frac{J_w}{k}\right)}{1 + \frac{B}{J_w}\left[exp\left(\frac{J_w}{k}\right) - exp\left(-\frac{J_w S}{D}\right)\right]} \right\} \quad (52)$$

$$J_w = B \left\{ \frac{C_D exp\left(-\frac{J_w S}{D}\right) - C_F exp\left(\frac{J_w}{k}\right)}{1 + \frac{B}{J_w}\left[exp\left(\frac{J_w}{k}\right) - exp\left(-\frac{J_w S}{D}\right)\right]} \right\} \quad (52)$$

In which, k,D are the feed solution mass transport coefficient and the bulk diffusion coefficient of thedraw solute. S is the structural parameter of the support layer membrane while $exp\left(\frac{J_w}{k}\right)$ and $exp\left(-\frac{J_w S}{D}\right)$describe concentrative external concentration polarization (ECP) and dilutive ICP. The previous water flux equation was rephrased including the non-linear equality constraint:

$$J_{w,i} - A\left\{\frac{\pi_{D,i} exp\left(-\frac{J_w S}{D}\right) - \pi_{F,i}}{1 + \frac{B}{J_w}\left[1 - exp\left(\frac{J_w}{k}\right)\right]}\right\} = 0 \quad (52)$$

In the last step, the algorithm was used considering the lowest E from three different solution concentrations. The coefficient of determination was also calculated based on this water flux equation:

$$R^2{}_w = 1 - \frac{SS_{err,w}}{SS_{TOT,w}} = 1 - \left(\frac{\sum_i^n = 1\left(J_{w,i}^{EXP} - J_{w,i}^{CALC}\right)^2}{\sum_i^n = 1\left(J_{w,i}^{EXP} - J_w^{-EXP,n}\right)^2}\right) \quad (52)$$

In which, SS_{err}, SS_{TOT}describe the residual sum of squares and the total sum of squares respectively. The coefficient of determination for the solute flux ($R^2{}_s$) was also calculated separately. Although water passage within the composite membrane is controlled by the physicochemical properties of the thin film, the support structure can also influence the mass transfer through the composite membrane. The membrane structural parameter (S) is an important element for a highly effective FO system. It verifies the extent of ICP. When S is high, this leads to increase the mass resistance and ICP, thereby decreasing the water flux [11, 53, 54]. The S is correlated to the thickness (t_s), tortuosity (τ), effective porosity (ε_{eff}) and solute diffusion coefficient (D) [5, 11]. It can be calculated using this equation [4]:

$$S = \frac{\tau . l}{\varepsilon} \quad (4)$$

Which can be re-expressed as follows:

$$K = \frac{S}{D} = \frac{t_s \tau}{D \epsilon_{eff}} \quad (10)$$

Where K denotes the structural properties of the membrane and solute diffusion coefficient,$D\epsilon_{eff}$ is the effective diffusion constant. Although water passage within the composite membrane is controlled by the physicochemical properties of the thin film, the support structure can also influence the mass transfer through the composite membrane. The porosity of the PSf substrate is important for the fabrication of various TFC membranes. Low porosity and large pores in the support layer are preferable to raise the water flux, whereas a highly porous substrate with narrow pores is required to improve salt rejection. Another major obstacle that affects the solute transport within the support layer is the presence of ICP effects. It has severe effects on the osmotic driven membranes. Thus, a significant reduction in water permeates might occur. It is likely the osmotic driving force could be decreased considerably due to external CP [5, 30 53], leading to a decline in water flux. In this case, the water flux can be described considering the effects of concentrative ECP and dilutive ICP as follows [53, 54]:

$$J_w = A\left[\pi_{D,b} exp(-J_w K) - \pi_{F,b} exp\left(\frac{J_w}{k}\right)\right] \quad (53, 54)$$

Where $\pi_{D,b}$and $\pi_{F,b}$represent the osmotic pressures of the DS and FS at the membrane surfaces respectively, k_{F} is the mass transfer coefficient of the feed. The reverse solute flux passes through the support layer, the dense active layer and the boundary layer. When it flows from the DS stream to the FS stream, this may reduce the osmotic driving force and induce fouling. This suggests a significant role of the sub-layer and therefore, these parameters can be improved by altering the casting conditions of the support layer such as composition and concentration or immersion precipitation conditions such as temperature and humidity during the fabrication of the support layer [4]. When the support layer is being synthesized, it is possible to control the structure dependent of the bulk and active layer separately. For instance, a thin and dense structure of the sub-layer can be obtained when adding a solvent to the coagulation bath.

Adjusting the temperature and incorporating an additive may result in modifying the tortuosity of the support layer. This can produce a desired finger-like structure leading to low S value. However, when there is agglomeration arising from the polymeric substrate, this can result in reduced salt separation or rejection by the active layer [55]. Given the recent research efforts that focus on adjusting the sub-layer structure to augment the mass transport, it is also important to explore whether these other alteration methods contribute to minimizing the impacts of ICP.

3 FO membrane advancement

Membranes specifically manufactured for FO use can be generally classified based on materials into CA/CTA membranes, TFC membranes, and biomimetic membranes. Also, chemically modified membranes have been widely used for the FO system. A diverse range of fabricated and chemically modified FO membranes is demonstrated in Table 1.

3.1 Cellulosic membranes

TFC RO membranes used in the FO process have shown low water permeability [56] due to the support layer being made of a mesh embedded dense porous mid-layer. This structure made the diffusion of draw solute difficult and the mass transfer resistance increased. Later, cellulose acetate membrane was synthesized by Loeb and Sourirajan [57, 58, 59]. It was the best class of membranes at that time, produced by Hydration Technology Innovations (HTI). It has superior advantages compared to other types, such as being easy to scale up because both the active and support layers were fabricated by phase inversion, and it has good hydrophilicity and mechanical strength [60]. Early studies examined the commercial cellulose acetate RO membranes in order to desalinate wastewater using the seawater as a DS. This CA membrane was used also for seawater desalination using the osmotic pressure produced from glucose solutions [59]. These

cellulosic membranes were reinforced using mineral additives to optimize their performance. However, the CA membranes produce low water flux and high salt passage and are prone to hydrolysis. McCutcheon et al [10] used a thinner cellulose acetate (CA) based membrane without a fabric support. FO membrane showed improved water permeability and a rejection rate of NaCl. Another class is CA hollow fibre from Dow which produced low water flux in the FO system [61]. Polybenzimidazole (PBI) nanofiltration (NF) hollow fibre membrane was fabricated by the common dry-jet wet phase inversion technique [62]. It is composed of double skins of active layers aiming to minimize the ICP effects [60, 62]. However, cellulosic membranes can be hydrolysed and are susceptible to bio-fouling [48, 63]. Regardless, the pH of solutions in the FO process is critical and should be set between 4 and 6 with a temperature lower than 35°C [30, 64]. In 1990, Osmotek Inc (currently HTI) patented advanced cellulose triacetate (CTA) based FO membranes with a thickness of 50 μm and supported by a fabric backing layer [5]. These membranes were employed in many applications including wastewater and seawater filtration. HTI was the first to develop CA/CTA membranes in flat sheet and hollow fibre configurations specifically designed for the FO process [60, 65]. It was realized that most of the scientists preferred using the CTA membranes rather than CA membranes to assess the membrane performance [10, 33, 66]. The HTI membrane composed CTA coated on a polyester mesh and the total thickness is (<50 μm) [67, 68]. The performance of the membrane involved good antifouling property due to low water flux during the fouling test using feed containing 0.01% (w/v) latex suspension. Later, Wang et al. [69] developed CA membrane, which consisted of a more porous mid-layer embedded between two active layers. The FO experiment indicated a high water permeability of 0.75 LMH and salt permeability of 0.25 against 100 ppm $MgCl_2$ feed. The water permeability was lower of 0.72 LMH using 5.0 M magnesium chloride ($MgCl_2$) feed, as a result of high salt passage or very low salt rejection of 79% for 100 ppm $MgCl_2$ and 58% 100 ppm NaCl in RO test.

An example of cellulose ester membranes is a balanced structure of a thin porous sub-layer and a thin dense active layer [70]. This membrane contained a sub-layer with a very low thickness of 30 µm which yielded a reduction in the ICP impact. Acceptable water flux was noticeable against a seawater feed and a 1.5 M NaCl draw solution. However, hydrophobic groups in this material may damage the active layer during the synthesis process [71]. Because of the aforementioned drawbacks, much interest was transferred to using a commercial flat sheet polyamide composite membrane. Scientists used either flat sheet or hollow fibre TFC-RO membranes for FO experiments. The first such membranes were fabricated by Cadotte in the 1970s [72].

3.2 Thin film composite membranes (TFC)

Flat sheet TFC-FO membranes were prepared by phase inversion of PSf support layer and cast on to a fabric backing layer followed by IP for the active layer [6, 56].In comparison with the TFC-RO membrane, the TFC-FO membrane is thinner, has higher porosity and hydrophilicity [45]. However, flat sheet membranes showed very low water flux because of a thick sub-layer that was induced by severe ICP impact [73]. A hollow fibre FO membrane was fabricated by the same method on either the external or internal surface of a polyether sulfone (PES) substrate [74, 75]. Interfacial polymerization was employed for preparing the polyamide on the support layer of the membrane. Oasys Water Company in collaboration with Yale University pioneered TFC-FO membranes for forward osmosis industry [75]. Owing to its finger-like structure and high porosity of the PSf sub-layer, the pure water flux increased to over 7 LMH while the salt rejection was as high as 97.41% using 500 ppm (8.6 mM) NaCl solution in RO test. This membrane performance outperformed the commercial HTI-CTA membranes.1.16 LMH using DI water and salt rejection of 94.1% using 50 mM NaCl feed in RO mode [11]. However, the sub-layer is thick and the structural

parameter (492 μm) needs optimization. Moreover, recent TFC-HTI membranes included a mesh-embedded sub-layer was synthesized. It exhibited 2 folds higher water flux (1.4 LMH) than commercial CA membrane but lower salt rejection of 92% [16]. The sub-layer thickness is double CA and it had a high S value of 533 μm. In addition, a flat sheet TFC made of both spongy skin and a finger-like structure produced a structural parameter of 670-710 μm. This may decrease the tortuosity, yielding to quite low ICP impact [29]. The water flux was higher than 12 LMH as compared to commercial CTA membrane (5 LMH) and a brackish water RO membrane (0.78 LMH) using 10 mM NaCl FS and 0.5 M NaCl DS. It appears that the straight finger-like pore structure is more significant than the sponge-like structure to mitigate the ICP. Presently, a hollow fibre membrane synthesized with double active layers on PES a sub-layer [76]. The sub-layer contained a dense and porous finger-like macrovoid structure, and S value was of 996 μm. In this case, the outer selective layer successfully minimized the ICP and fouling into the sub-layer against real wastewater brine. This new membrane had acceptable mechanical strength for hydraulic pressure over 20 bar and superior fouling resistance. An excellent water permeability of 1.5 LMH and a very low salt permeability of 0.02 LMH and a salt rejection of 94.2% were recorded using DI water and 1000 ppm NaCl FS respectively.

In summary, other players in the market include Porifera, Toray and Aquaporin. The TFC membranes performed better than cellulosic membranes because of higher tolerance to pH ranges from 2 to 11 and were stable at a temperature over 60^{o}C. As mentioned previously, it exhibited higher water permeability and can tolerate the process conditions of pressure retarded osmosis (PRO) [77]. In contrast, the two stages of preparation result in higher cost and there is a challenge in controlling the IP process of the selective layer. The performance of hollow fibre is sometimes restricted by fouling and pore blocking of the narrow inner diameters. It is ineffective for treating industrial wastewater, as well as low amounts of fouling agents [45].

3.3 Biomimetic membranes

Commercial Aquaporin embedded TFC membranes are produced by Porifera[78], which are made of aquaporin water channels that are incorporated into the selective layer of hollow fibre membranes [79]. They show excellent chemical resistance for cleaning agents such as NaCOl, HCl, SDS and Alconox with a pH that ranges from 1.4 to 11.7. After chemical cleaning, a considerable increase in the water flux and salt rejection was achievable [80]. This membrane showed increased water permeability from 2.85 LMH to 3.66 LMH and a comparably low salt permeability of 0.36 LMH versus 0.31 LMH. In fouling tests using secondary wastewater effluent FS and seawater DS, the flux was declined at 4.6 LMH but it was still higher than commercial CTA membrane (3.4 LMH). This can be ascribed to the fouling layer on the membrane surface. Along with this, a high rejection for salts (99%) and for dissolved organic carbon (average 90.7%) over 15 days was reported. However, chemical cleaning may affect the aging of the membrane over long-term operations. As such, the sub-layer thickness is critical; it can be adjusted by chemical treatments to further improve the membrane performance.

3.4 Chemically prepared membranes

Polyelectrolyte multilayer (PEM) was used to synthesize FO membranes. One of the advantages is the thickness can be controlled to nm as well as the charge density which is convenient to enhance water permeability and separation properties [81, 82]. The process is illustrated in Fig. 4(a), where the negatively charged substrate exposed to polycation (PAH) is first rinsed in water followed by the polyanion layer (PSS) and again rinsed in water. FO membrane made via L-b-L was by Setiawan et al. [83]. This Polyamide–imide (PAI) hollow fibre membrane with NF-like selective

layer was synthesized by a multilayer of polyelectrolyte. The water permeability was very low at 2.19–2.25 LMH, whereas the salt rejection exhibited 49% and 94% for NaCl and $MgCl_2$ respectively. Later on, the hollow fibre membrane was prepared by subjecting the external surface of the membrane to polyelectrolyte post-treatment [84]. The external surface got rougher while the morphology maintained its thin sponge-like structure in the middle and thin fibre wall to reduce the ICP. It was achieved high water permeability of 3.7–4.3 LMH. The salt rejection was up to 85%. Another type is PAI-PES dual-layer NF-hollow fibre synthesized via further multilayer polyelectrolyte deposition [85]. After the PEI deposition on the hollow fibre membrane, the morphology was retained but the external surface became rougher. It is confirmed that this membrane exhibited higher water permeability of 4.1 LMH and greater salt rejection of $MgCl_2$ up to 97% against 500 ppm $MgCl_2$ solution in RO test. The salt flux was very low at about 0.08 LMH.

A flat sheet polyamide-imide (PAI)-FO membrane was exposed to polyelectrolyte (PEI) post-treatment. This membrane achieved superior water flux of 19.2 LMH and the selectivity ratio (J_s/J_v) of < 0.5 g L^{-1} utilizing DI water FS and a 0.5 M $MgCl_2$ DS [86]. Moreover, the NF-FO membrane was synthesized via this treatment, aiming to reach the maximum magnesium chloride ($MgCl_2$) rejection rate [87]. To improve the ionic bonding of the first layer, the substrate was pre-treated by sodium hydroxide (NaOH). It was observed that the uppermost surface was smooth and uniform while the bottom surface contained big pores. The resultant structural parameter was 0.5 ± 0.2 mm which is lower than that for the commercial HTI membrane (0.7-1.4 mm). When six multi-layers of polyelectrolyte were applied on the surface, the water flux declined but the selectivity was enhanced significantly with reduced salt leakage. The best water permeability approached 52.3 $X10^{-11}$m/s Pa for membrane treated NaOH but it was decreased for membrane with more layers of this treatment. It appears that #3 L-b-L modified membranes showed higher water permeability at 2.8 $X10^{-11}$m/s Pa than that for #1 L-b-L and #6 L-b-L. Conversely, the salt

permeability was better of $3X10^{-7}$m/s and salt rejection was of 80% for #6 L-b-L. Overall, the salt permeability and salt rejection were enhanced when applying more layers of L-b-L when using divalent $MgCl_2$FS.

Liu et al [88] synthesized the FO membrane by a different method, including assembling multiple polyethylenimine (PEI) and sodium alginate (SA) bilayers over a polydopamine-treated polyvinylidene fluoride (PVDF) substrate. When more layers were applied on the substrate, the water permeability and salt passage were lowered corresponding 1.27 LMH and 0.03 LMH respectively. The salt rejection was better than that for #1 and #3 L-b-b approaching 96.8% using 10 mM $MgCl_2$ in RO experiment. The highest metal rejection was reported for the membrane with 3 polyelectrolyte layers estimated by > 99.31% in FO process using 2 g/L heavy metal ions FS and 1 M $MgCl_2$ DS. It is most likely because a thicker skin caused great salt flux resistance. Even though membranes prepared via this method have high thermal stability, excellent solvent resistance, and stable cross-linking, it is time-consuming to produce the new membrane [82, 89]. It involves a complex synthesis procedure and is expensive for large operations which restrict its commercialization [28]. The difference in surface roughness and the formation of defects and a loose selective layer are challenging [90, 91]. It is also important to understand the structure and properties of the FO membrane in order to evaluate the ultimate performance. Further improvements are needed to fabricate a thinner and porous sub-layer with more interconnected pores and less tortuosity to maximize the membrane productivity.

3 Improvement in fabrication procedures for FO sub-layer

4.1 Sub-layer modified via phase inversion

The phase inversion method depends mainly on the de-mixing of a polymer solution and phase separation to create a porous polymeric membrane [92]. Therefore, the morphology of the

support layer depends on the dissolution between solvent-nonsolvent and between polymer and non-solvent. The exchange between solvent in the polymer solution and non-solvent from the coagulation bath results in the de-mixing and precipitation of so-called non-solvent induced phase separation (NIPS) [93, 94, 95, 96]. It was reported that some parameters can impact the morphology and pore-forming of the membrane. These parameters are kinetic properties composition, a temperature of the polymer solution, additives, and a coagulation bath. When a rapid de-mixing of the polymer occurred due to the high thermodynamic aspect, a skin layer of the membrane can be produced quickly [92]. The formation mechanism of morphology depends on adjusting the solvent and non-solvent ratio during the synthesis process to control the thermodynamic and kinetic aspects. The properties of additives into the polymer matrix are significant because they may impact the thermodynamic (affinity with solvent, non-solvent, and polymer, also solvent-non solvent solubility) and kinetics (high viscosity of the casting solution) of the preparation step [92]. The final structure comprises macrovoids or porous structure in the PSf support layer while a dense skin is formed on the top.

Since a thin, porous and less tortuous sub-layer is necessary to obtain a low structural parameter, this can be achieved through lowering the concentration of the synthetic polymer and using various additives [56]. A hollow fibre membrane was prepared via phase inversion and the inner substrate modified by adding PVP solvent [97]. This modification showed a spongy structure in the inner substrate due to delayed de-mixing during phase inversion. Importantly, it inhibited the formation of delamination caused by incompatibility between the inner and outer layers.

Hajighahremanzadeh et al [98] used a low amount of PAN polymer (7 wt %) and the coagulation bath temperature was adjusted to 0^{o}C. The resultant flat sheet sub-layer showed a relatively thin and dense skin of 84.0 µm, a more porous structure of 90.1% and broad channels with thin walls.

In the RO test using 2 g/L NaCl feed solution, the A value achieved 1.13 LMH and B was very low at 0.335 LMH. This is because of reduced S and τ values of 112.1 µm and of 1.21 respectively. In comparison, Wu et al. [99] used polyethylene glycol (PEG)-400 with a concentration of 6 wt.% as a pore forming in the casting PSf polymer solution. A flat sheet sub-layer was produced, having 51 µm thickness but less porous at 84%. The S value declined considerably from 434 to 182 µm, indicating reduced ICP impacts. When a higher salinity of NaCl DS (2.0 M) was used, an improvement in the A and B values was observable, approaching 1.55 from 0.99 LMH and 1.16 LMH respectively. The polymer composition, the nature of solvent and non-solvent, the coagulation bath, and the interaction mechanism between polymer and casting layer can also impact the morphology and pore-forming of the fabricated membrane [57, 100, 101]. Adjusting the solvent and non-solvent ratio during the synthesis process may control the thermodynamic (affinity with solvent, non-solvent, and polymer, also solvent-non solvent solubility) and kinetic (high viscosity of the casting solution) aspects may provide the desired sub-layer morphology.

Lu et al [102] used DMF solvent instead of NMP for synthesizing the PSf sub-layer of TFC membrane. The DMF-TFC membrane showed bigger pore size and a higher porosity of 1.99% than that for NMP-TFC membrane of 1.01 %. Although the S value of the former was increased (953 µm versus 817 µm), its large surface area allowed high water permeation. Thus, the A value was higher at 3.14 LMH for DMF-TFC membrane versus 1.73 LMH for NMP-TFC membrane. However, the former showed slightly higher B value at 0.60 LMH versus 0.50 LMH for the latter.

Tiraferri et al [56] observed that a mixed solvent process and lower PSf polymer concentration of 9% in and 100% DMF caused a drop in S value from > 2000 to 312 µm. In the RO test using simulated brackish water (50 mM NaCl), the water permeability was increased of 1.9 LMH whilst the salt permeability was 0.33 LMH, and the salt rejection reached 98.6%. He suggested that the

mixed structure of more porous finger-like macrovoids in the sub-layer may show less mass transport resistance, while a thin sponge-like structure on the uppermost surface of the support layer might produce high permeable FO membrane.

Li et al [103] added LiCl pore forming additive into polyetherimide (PEI) substrate of TFC hollow fibre membrane. It was found that the morphology of the substrate contained a uniform finger-like structure, thicker skin layer, and low mean pore size of the inner surface. However, the porosity was unchanged while the membrane walls became slightly thinner. This is due to delayed de-mixing during the phase inversion process leading to narrowing of the macrovoids. It was also the prevailing view that this additive caused a collapse of the macrovoid, a reduction in pore size and porosity due to slow phase separation at high content of this additive [104]. The tortuosity of the new membrane was reduced resulting in lower S value (from 308 to 254 μm). This caused an improvement in water flux of about 31.8 LMH, A value of 3.44 LMH and B value of 0.4 LMH versus pristine TFC membrane (25.4 LMH, 2.85 LMH, 0.36 LMH) in FO mode against DI water and 1 M NaCl.

Liang et al [105] proposed using the PI combined bidirectional freezing process to tailor the PVDF substrate of a TFC membrane. It was chosen to make a substrate with vertically oriented pores in the sub-layer. The preparation process is illustrated in Fig. 5(a) so the polymer solution was added into a mould made of two stainless steel and glass plates [106]. Then the thickness was tailored perfectly and the mould was located in a water bath with various temperatures. Next, it was soaked vertically in an extraction solvent to obtain the membrane containing vertical pores. The newly developed FO membrane showed a nodular structure on the top and its porosity was estimated at 74%. It can be seen from Fig. 5(b) that the pores were formed vertically with a pore size of about 1.8 μm. It can be observed that pores have an open shape in the bottom and top

sides, as well as a spongy structure in the midlayer as shown in Fig. 5(b). Thus, this sub-layer structure had an excellent low tortuosity and a low S value of ~100 µm. This novel substrate achieved higher A value by 4 folds (4.7 LMH) versus PI-TFC membrane having an A value of 0.63 LMH.

4.2 Sub-layer modified via Electrospinning

The electro-spinning process produces polymeric fibres with a diameter between 5 to 500 nm and less than several micrometres, a small pore size and large surface area [107, 108]. The scaffold-like nanofibers can be transformed to more porous with interconnected pores to obtain low tortuosity and S value [109]. Compared to PI technique, this structure can be obtained easily by the electro-spinning method [110, 111]. The morphologies, orientation of prepared nanofibre, different diameters and aspect ratio can be fulfilled by controlling the environment conditions, the solution viscosity, the flow rate of the solution, and the applied voltage [112].

Song et al [109] tailored a PES nanofiber sub-layer via electro-spinning for the FO process. It was easy to control the thickness of nanofibers by adjusting the temperature, resulting in diameters ranging between 50 and 150 nm. This nanofiber support exhibited a special porous structure, scaffold-like, with tight pores among single nanofibers. As a result, the S value was very low, it involved high porosity, low tortuosity and salt diffusion resistance of the support layer. This nano-fibrous support of FO membranes achieved satisfying results in both FO and PRO systems.

Bui et al [113] promoted the polymer composition properties by blending polyacrylonitrile (PAN) and CA polymers to prepare the nanofibrous substrate. It was observed that a homogenous and uniform nanofibrous substrate with hollow peaks nanoporeswas attached strongly to the selective layer. In Fig. 6(a), (b), (c) and (d), the fibres appeared fine and uniform and then they

became larger when increasing the concentration of PAN. This resulted in high viscous polymer solution leading to large diameter and big pore size. Fig. 6(e) and (f) showed a good compatibility between the nanofibrous layer and the selective layer, displaying a total thickness of 10-15 µ. Interestingly, this substrate with polyethylene terephthalate (PET) backing layer demonstrated reduced S value from 693.2 to 290.7 µm. The A and B values were increased to 2.036 LMH and 1.572 LMH respectively as compared to commercial HTI-CTA membrane (A = 0.683, B= 0.340) when using 2000 ppm NaCl FS in the RO test.

Another useful design for FO substrate is a fine and thin nanofibrous upper layer compatible with the selective layer and rougher fibres in the bottom to improve the substrate strength. Tian et al [111] fabricated a polyetherimide (PEI) nanofibrous substrate that embedded functionalized multi-walled carbon nanotubes (f-CNTs). Due to the homogenous dispersion of f-CNTs, substrate tensile strength and stiffness were enhanced significantly. Besides, the porosity rose from 59% to 81%, showing perfect interconnected pore structure. This morphology yielded a reduction in S value from 674 µm to 310 µm which hindered the ICP effects. Compared to TFC-HTI membrane having A= 1.63 LMH and B= 0.3 LMH, this potential substrate accomplished a superior A value of 2.6 LMH and a little increase in B value of 0.7 LMH.

Bui and McCutcheon [114] prepared a nanofibrous substrate by impregnating 15% mesoporous silica nanoparticles into polyacrylonitrile (PAN) nanofibrous substrate. The nanoparticles were well distributed in the substrate, providing additional water pathways via the particles' porous channels and improved water holding capacity. Hence, the S value was declined greatly from 229 to 65 µm. Consequently, the altered substrate achieved an outstanding A value of 2.54 LMH but the B value was greater at 1.66 LMH against HTI-CTA membrane having A= 0.66 LMH and B = 0.44 LMH, using DI water and 2000 ppm NaCl feeds in the RO system. The salt permeability declined

as a result of silica clusters on top of the nanofibrous substrate which may influence the active layer efficiency. There was no significant change in the tensile strength of the membrane. From these works, it can be recognized that nanofibrous membranes might have potential advantage over classical membranes fabricated by the PI method. Due to their special design containing narrow pore size, highly porous and interlinked pore structure, the ICP reduced significantly. This allows the free diffusion of the solution in the sub-layer leading to enhancement in water permeation through the selective layer. Despite its favourable characteristics, the high porosity may cause a serious increase in salt flux for some developed membranes [110]. Importantly, these membranes could have insufficient mechanical strength [115, 116] to withstand an applied pressure when measuring the intrinsic performance parameters for large scale operations. The preparation procedure is complex and takes a long time. There is still a critical issue encounter in compatibility between the nanofibrous substrate and the selective layer [116].

5 Current challenges for FO membranes

The most significant challenges are relevant to these factors: membrane design, draw solute characteristics, concentration polarization, reverse salt flux, and membrane fouling. Membranes are the heart of an effective forward osmosis process. Asymmetric membranes have been seen in the past to exhibit weak performances in FO processes [44]. The porosity of the support layer influences mass transport resistance, salt precipitation, and ICP within the porous structure. The change in the pore structure of the support layer may further affect the permeability of the thin film formed on the top [117, 118]. It was suggested that the chemistry and pore structure of the

support layer can alter the morphology of the selective layer. This implies a clear correlation between surface morphology, the structure of the support layer and the selective layer performance. It is generally accepted that the surface porosity may lead to variability in the structural parameter of the FO membrane. A large number of studies have addressed the issue that the micro-porous support layer can limit the mass transfer leading to severe ICP [2, 48, 54, 57, 66, 119, 120, 121, 122]. The ICP is a critical factor that influences the performance of FO membranes. This is because the concentration polarization (CP) effects appeared not only throughout the boundary but also across the membrane surface as a result of non-ideal hydrodynamics. According to Zhao et al [30], the dilutive ECP occurs when the sub-layer is against the feed solution. To avoid the impact of ECP on the water, it should be increasing the flow velocity or turbulence or optimizing the water flux. Conversely, it is difficult to eliminate the severe effects of ICP by changing these operating conditions [30]. The ICP can be influenced by the membrane porosity, thickness and pore tortuosity. Another important factor is the draw solution properties because if the concentration of DS was reduced within the dense support layer, the ICP may result in poor water flux and salt leakage [4, 54].

Other technical obstacles include the reverse solute flux which appears unavoidable in the FO process, particularly for small draw solutes, because of the concentration difference between the feed and draw solutions. Zhao et al [123] addressed the fact that there is a strong relationship between fouling and the reverse diffusion of the draw solute when using organic macromolecules and colloidal particles, for example, in plate and frame configuration. When fouling occurs because of the accumulation of various components on the surface of the membrane or deposits within the pores, this yields a pore blocking [80, 123, 124]. Compared to the RO system, the fouling in the FO process is reversible because of induced cake-enhanced osmotic pressure (CEOP) [30]. He reported that this issue was caused by reverse salt flux from the draw solution. In other

words, reverse solute flux may aggravate the CEOP in the fouling layer. Consequently, the elevated osmotic pressure opposite the feed side caused a decline in the net osmotic pressure, leading to a serious drop in the water flux [125]. However, there is limited research reported on mitigating the fouling of FO membranes.

Moreover, one of the most critical issues is the characteristics of the FS and DS. For instance, the viscosity and concentration of the DS should be optimized to prevent ICP effects that results in poor membrane performance. To avoid the effect of salt back diffusion, enhancing the selectivity of the membrane is also essential. Without a suitable membrane, it is difficult to materialize FO as a feasible desalination technology. Therefore, the ideal support layer should be thin, highly porous, and allow easy passage of water in order to improve the membrane permeability. The perfect FO membrane should exhibit low ICP, be highly permeable, antifouling, be chemically stable, demonstrate prolonged stability in terms of mechanical strength and have a minimal reverse solute flux [126, 127]. Because of these restrictions, research is needed to modify the FO membrane structural properties and to promote the ultimate performance. Recognizing the extent to which the sub-layer structure might influence the mass transport would also need efforts devoted to promoting the ultimate performance which will contribute to real world implementation.

6 Advanced chemical modifications of the synthetic polymer

Many significant improvements have been made to TFC membranes intended for use specifically in the FO system. Research into TFC membrane modifications can be classified into physical and chemical modifications. Here, the second category will be the main approach for the following sections. The modification of the polymer can be divided into alteration of the synthesis

conditions and blending of the base polymer with other additives. The bulk modification of the polymer is useful to transform polymer from hydrophobic to hydrophilic, and to integrate hydrophilic material into the pores, leading to enhanced water flux, antifouling property and overall compatibility [30]. A wide range of polymers have been used to fabricate FO membranes, such as PSf [11], polyethersulfone (PES) [64], polyamide-imide (PAI) [84], CA [128] and PBI [129, 130]. The polymer matrix properties can be modified by acidic agents before incorporating polar additives into the polymer matrix during the preparation step. The aim of this chemical modification is to increase the hydrophilicity of the support layer which is crucial to the water permeability and salt rejection of the TFC membrane. It was elucidated that when the PSf support layer was made hydrophilic, the water flux and salt rejection was enhanced significantly [121].To produce good membrane performance, sulfonation, carboxylation, and nitration for PES polymer were examined. The most common polymers used to prepare FO membranes are sulfonated poly(phenylenesulfone) (sPPSU), sulfonated PSf (sPSf), and sulfonated poly(ether sulfone) (sPES). Besides, the fabrication via chemical modification involves the incorporation of polymer additives or inorganic nanoadditives, such as nanoparticles/nanomaterials to provide a higher hydrophilicity and effective membrane performance [119, 131, 132].

The first section will discuss the chemical modification or bulk modifications of the synthetic polymers. There are few works in the literature on the chemical modification methods of the synthetic polymers. The effects of these methods on the morphology and the membrane performance are briefly discussed below.

6.1 Sulfonation process

Sulfonation involves the addition of sulfonic acid groups (SO_3H) into the membrane polymer matrix. This chemical interaction results in replacing hydrogen atoms by sulfonic groups, namely electrophilic reaction [36]. Earlier works focused on the sulfonation of PSf for pervaporation separation [128, 129] and sulfonated PES for gas separation [133]. To promote the base polymer hydrophilicity and therefore enhance the FO sub-layer productivity, PSf/PES was functionalized by the sulfonation method. In contrast, the application of sulfonated polymer, prepared by this reaction, suffered from having a heterogeneous structure and disintegration [134]. It should be noted that the hydrophilization treatment by sulfonated polymer may influence the mechanical properties of the support layer because of a high swelling ratio when it came into contact with water [135]. Along with this, the swelling of the polymer would lower the rejection rate of the membrane [30]. Researchers have studied the chemical functionalization procedures, including sulfonation, carboxylation, bromination, and acylation which can be applied to increase the "upper-bound" limit correlation between permeability–selectivity [133].

6.1.1 Sulfonated polysulfone polymer (PES/sPSf)

The chemical modification of PSf has been observed to contribute to the improvement of FO membrane performance [136]. One study used PES/ sPSf support layer, with the interfacial polymerization process to synthesize a polyamide film active layer [136]. The structure of the substrate is composed of a thin and dense film on the surface and a porous mid layer. In spite of this, the PES/sPSf substrate exhibited small pore size, almost unaltered porosity, and an average pore size around 12.8 nm but with a large pore size distribution. The hydrophilicity was improved significantly. The RO filtration test showed the water permeability of 0.77 LMH and salt flux of 0.11 LMH which are lower than PVDF membrane (0.82 LMH and 0.19 LMH). The salt permeability

was measured against 1000 ppm NaCl in RO test. In FO test, there was a decrease in the water flux because of severe ICP through the porous support. At high salinity, the osmotic force was declined, leading to a nonlinear relationship between water flux and salt concentration. The ECP at the interface of the membrane surface and ICP in the membrane contributed to the drop in the osmotic pressure across the active layer. Besides, the salt flux was increased when high DS concentration was used in FO mode. It was concluded that both the structural parameter and the fabrication procedure have major roles in managing the membrane performance.

6.1.2 Sulphonated polyethersulfone polymer (sPES)

Membranes incorporating sPES have been frequently utilized in FO desalination. PES is a thermoplastic material composed of ether and sulfone groups and has perfect mechanical and flexible behaviour, thermal stability, hydrophobic skin with desired properties, and high glass transition temperatures [137, 138].

It is generally recognized that the sulfonation of a polymer improves the hydrophilicity along with alteration of the substrate morphology. Many scientists have studied this process and each author found out different results depending on the sulfonation degree and the materials used. For example, Sahebi et al [139] reported that with a high degree of sulfonation (50 wt.%), the structure was modified from a finger-like structure to a thinner spongy structure. The porosity and hydrophilicity were enhanced and a lower structural parameter of 245 µm was achievable. The water permeability was increased reaching 2.9 LMH for 50 wt.% sulfonated material embedded membrane using DI water in RO test. However, the salt permeability was moved up to 5.1 LMH from 2.6 while the salt rejection was acceptable of about 91.1% against 200 ppm NaCl in RO test. This can be ascribed to the sulfonic acid connected to the polymer chain and lower

agglomeration of the polymer became more flexible. The developed membrane outperformed the TFC-FO pristine membrane under the same conditions.

When Wang and Xu [140] blended hydrophilic SPES with Montmorillonite (MMT), similar results of hydrophilicity and finger-like pores and spongy structures were observed. The purpose of adding MMT was to stabilize the hydrophilic polymer in the suspension during the fabrication of TFC-FO membranes using the NIPS method. The hydrophilicity was improved because the sulfonic acid replaced the hydrogen atoms in an electrophilic interaction. The advantages are a decrease in the ICP, reduced structural parameter of 0.79 mm and enhanced flow of water flux. Consequently, the highest water permeability of 1.2 LMH and lowest solute permeability of 0.8 X 10^{-8} m/s for MMT embedded SPES having sulfonation degree of 40%. As a result of high hydrophilicity and a tight pore size distribution. Despite that, the selectivity was retained because the thickness of the sponge-like structure could impact the mass transport of the flux within the membrane. All of these modifications can be restricted by the dispersion rate of the modified polymer in a non-solvent, while Guan et al [35] used chlorosulfonic acid and sulfuric acid solvent to produce sPES via a homogeneous method. The hydrophilicity was enhanced, as seen by contact angle measurements. When the degree of sulfonation was 40%, the water holding capacity suddenly increased. In contrast to the above studies, sulfonation can influence the mechanical strength of the prepared polymer. Subsequently, the structure of the resulting sPES membranes contained inclusions in the matrix due to the presence of the sulfonic acid groups at higher degrees of sulfonation. There was a considerable decrease in the polymer breaking resistance.

6.1.3 Sulfonated polyphenylenesulfone (sPPSU) polymer

The degree of sulfonation is a significant factor, which may impact the water holding capacity and morphology of FO membranes. In the past, the sulfonation process was used to functionalize polysulfone polymer to obtain a high hydrophilicity, produce the desired macrovoids, open pore structures and to enhance rejection of organics [141, 142], leading to improved water fluxes in forward osmosis systems. In one study exploring the impacts of a sulfonated copolymer composed of PES and PPSU when blended with polyethersulfone (PESU E6020P) in a TFC membrane, it was found that the higher concentration of the sulfonated polymer in the substrate lead to lower surface roughness [143]. When 50 wt.% sulfonated material was embedded in the support layer, a more favourable sponge-like structure free of macrovoids was formed. The porosity and pore size increased due to slow de-mixing in the phase inversion compared to pure PESU. The structural parameter exhibited a low value of 3.24 X 10^{-4} m when increasing the amount of sulfonated polymer and therefore reduced ICP effects. Another advantage of this modification was the formation of a high permeable active layer on the substrate. In addition to this, the effect of directly sulfonated polymer with various sulfonation degrees on the morphology, mechanical properties and performance were investigated. It is important to note that the greatest water permeability approached 0.73 LMH for 50 wt% sulfonated polymer embedded membrane as compared to pristine PESU membrane because of improved hydrophilicity. The salt rejection and solute permeability almost remained the same when using 400 ppm NaCl solution in RO experiment.

When Widjojo et al [144] used sPPSU mixed with different monomers to fabricate the support layer, the thickness of both the non-sulfonated and sulfonated polymers was in the range of 35–50 µm. The sulfonated support layer was hydrophilic and had a sponge-like structure compared to the non-sulfonated sample with macrovoids only. A reduction in the ICP and a good wettability of the sub-layer were observable. When the polymer contained 2.5 mol% of 4,4'-Dichlorodiphenyl

sulfone, the membrane displayed very low water permeability of 3.23 LMH and salt passage of 1.05 LMH against DI water and 400 ppm NaCl feeds in RO filtration. In contrast, the pristine membrane showed water permeability of 12.53 and higher salt passage of 5.78 LMH. Interestingly, the salt rejection of the developed membrane was improved of about 84.1% versus the pristine membrane (81.7%).

In Zhong et al's [145] study, interfacial polymerization was adopted to prepare PPSU-TFC based hollow fibre membrane. It was found that the sulfonation preparation greatly influenced the membrane microstructure. This is because nonsulfonated membrane formed a macrovoid-free structure caused by quick de-mixing whilst the modified substrate (1.5 mol% sPPSU) displayed a sponge-like structure. The structural parameter was dropped to 1.63×10^{-4} m from 7.46×10^{-4} m for a pristine PPSU membrane. This allows more effective water diffusion within the membrane resulting in higher water permeability of 1.99 LMH, reduced salt passage of 0.0399 LMH and acceptable salt rejection of 90.9% against DI water and 1000 ppm NaCl in RO mode.

Nevertheless, the sulfonation procedure has some limitations, for instance, it is challenging to control the sulfonated group's location or the degree of the reaction which limits the simplicity of preparation and reproducibility [64, 146]. High swelling phenomena of PES and PPSU copolymer blended PESUE6020P causes a decrease in the pure water permeability [143]. According to Mockel et al [147], sPSf polymers with a high sulfonation degree are susceptible to swelling. This decrease in the mechanical strength of the resultant sPSf or sPES support layer might be caused by the higher concentration of sulfonated material due to a random distribution of the sulfonic acid groups on the polymer skeleton and decreased water uptake capacity [148]. It should be pointed out that this sPPSU copolymer has not been utilized extensively in the industry because of aggregation in the suspension during preparation [149].

6.2 Carboxylation process

The carboxylation modification process involves the deposition of a carboxylic group into the polymer backbone to enhance the membrane water uptake and hydrophilicity [137]. In comparison to sulfonation, carboxylation uses a weak acid, therefore swelling is absent even if the ion exchange capacity is increased. As reported by Cho et al [149], there is no change in the mechanical properties of the newly fabricated carboxylated PSf (CPSF), compared to pristine PSf. Research shows a difference in the performance of the carboxylated polyether sulfone (CPES) sub-layer for a hollow fibre membrane and that for a flat sheet TFC membrane, depending on the membrane type and the fabrication strategy. Wang et al [150] first functionalized the carboxylic polyethersulfone (CPES) by two reactions involving acetylating and oxidizing. The fabrication methods were blending and dry–wet spinning to produce hollow fibre membrane. The objective was to study the structure, performance and the surface physicochemical properties of the new fabricated membrane. Accordingly, it was clear that a thin skin formed on the internal and external walls of the hollow fibre membrane. The finger-like structure was predominant between the thin layer and pores while a rounded pore structure was observed. This structure was caused by the rapid mixing during liquid–liquid phase separation or it might have been a result of polymer aggregation and the spinning parameters. The membrane displayed a low water contact angle and showed pH sensitivity and reversibility. In contrast to the previous study, a sponge-like structure in the porous support of TFC flat sheet was observable [149]. This structure was changed due to the impact of the solvent and degree of substitution (DS). In Fig. 7(a), the preparation process is described clearly. Fig. 7(b) is illustrated the structure that transformed to a sponge-like structure in the microporous CPSF. As a result of high degree of sulfonation, more macrovoids

were created. The porosity and thickness of the support layer were increased which resulted in a higher structure parameter than PSf membranes. The reason was put down to more swelling at high acid concentrations during the phase inversion process. However, a positive impact is that the hydrophilicity was enhanced due to the polarity of carboxyl groups, suggesting low ICP effects. The hollow fibre membrane showed flux permeation rates to increase with higher concentrations of CPES. In RO mode using DI water, the pure water flux of the developed membrane was as high as of 2500 LMH for CPSF65 membrane prepared in 15 wt% DMF organic solvent versus 500 LMH for pristine PSF membrane. More importantly, the developed membrane exhibited enhanced protein antifouling properties. This method has a positive impact on the wettability, water adsorption, tensile stress, and the intrinsic structure.

6.3 Copolymerization process

There are many obstacles facing researchers using the sulfonation process to synthesize membranes. Thus, Harrison et al [151] developed an alternative method denoted as “directly copolymerized sulfonation.” The objective of this process is to control both the level of sulfonation and the sulfonic group position to produce homogenous sPSf incorporated material with enhanced reproducibility. It was confirmed that membranes formed via copolymerization have high resistance to chlorine at various pH values between 4 and 10, high protein and oil fouling resistance and acceptable performance [64]. The polyoxadiazoles (PODs) and polyazole−polytriazoles were used to prepare the FO membrane [152]. The former was selected because it has high oxidative, thermal and chemical stability but had high hydrophopicity. The latter had higher polarity, toughness, chemical resistance and thermal stability which made them strong candidates for the FO sub-layer.

Duong et al [152] pioneered the use of hydroxyl modified PTA-POD copolymer for FO membranes. One of the findings in this work is that 40 mol% PTA was the ideal concentration in 18 wt.% PSU polymer for TFC membrane, providing low ICP. The support layer was more porous with porosity of 74.4% and had tight pores with finger-like macrovoids. The lowest S value was reported for 40 mol % PTA–TFC membrane achieving 236 µm. The hydrophilicity of the sub-layer was significantly improved. The thickness was increased due to high amounts of hydroxyl-functional PTA leading to high structural parameter of 630 µm for 50 mol % PTA–TFC membrane. In the RO test using DI water, there was a slight decline in water permeability from 1.983 LMH for pristine membrane to 1.308 LMH for the new membrane. The salt rejection became high with increasing proportions of hydroxyl-functionalized PTA. When 2000 ppm of NaCl FS was utilized during the RO experiment, a high salt rejection of 94% was measured. Also, a very low salt passage corresponding to 0.285 LMH was observable. To that end, the homogenous dispersion of the solvent with the POD, minimum defects on the pore structure and strongly interconnected pores of TFC are necessary factors to control the salt separation property.

Another researcher indicated a repulsive force between the membrane surface and proteins suggesting enhanced organic fouling resistance [153]. In addition, this modified sub-layer outperformed a PSf-based TFC-FO membrane under the same experimental parameters in terms of antifouling/biofouling, protein rejection, and performance demonstrating a high potential for use in FO membranes. Nevertheless, some obstacles often encountered during the preparation of polyoxadiazole are low dispersion at high concentration and less mechanical stability. There are evidently more materials for FO membranes reported in other studies.

6.4 Incorporating hydrophilic polymer additives

More recently, sulfonated polymers were incorporated into the polymeric sub-layer to enhance its hydrophilicity along with the morphology, contributing to great membrane performance [154]. It has potential due to its hydrophilic nature, thermal stability, good mechanical characteristics, ability to scale-up and chemical resistance [154, 155]. As mentioned above, direct addition of sulfuric acid into the synthetic polymer caused swelling and less hydrolytic stability, particularly at high degrees of sulfonation. To avoid swelling problems, a cross linker such as a α, ω-dihalogenoalkanes agent was used to connect a sulfonate group into the backbone of a PSf via a cross-linking method [155]. This means the sub-layer can absorb a high amount of water in the presence of excessive sulfonic groups and high temperatures. Thus, high proton conductivity might be achieved because the water carriers in the membrane were able to hold more protons [109]. Another hydrophilic polymer with high proton conductivity is sulfonated poly(ether ether ketone)s (sPEEKs) [156].This probably contributed to high hydrophilicity and high water flux through the membrane.

Other polymer additives such as sulfonated poly(ether ketone) (SPEK) polymer, disulfonated poly (arylene ether sulfone), and perfluorosulfonic acid (PFSA) were contributed to good hydrophilicity in the newly developed FO support layer [148, 157, 158]. The major difference is that when the concentration of the deposited polymers is varied, the resultant sub-layer exhibited different morphology. For example, an SPEK embedded PSf sub-layer formed a sponge-like structure, and a lower structural parameter for TFC-FO membranes [157]. It was found that 50 wt.% was the optimal SPEK concentration in the sub-layer corresponding to a contact angle of 59.4^{o} due to the presence of sulphonic groups. Sequentially, the structural parameter was reduced of about 1.07 X 10^{-4} m versus pristine membrane with 1.82 X 10^{-4} m and hence suppressed the impact of ICP. In RO test utilizing DI water and 200 ppm NaCl feeds, the developed membrane exhibited little increase in the water permeability around 0.75 LMH, lower salt rejection of about 89.5%, and salt

permeability around 0.068 LMH for 50 wt% SPEK embedded membrane. Compared to pristine membrane, the water permeability, salt rejection and salt permeability were 0.5 LMH 91%, and 0.041 respectively.

Researchers showed different results when a PFSA introduced into PVDF sub-layer. The result indicated that a thinner and straighter finger-like structure could reduce the membrane tortuosity [158]. It was explained that the presence of $–SO_3$ groups in PFSA facilitated the mass diffusion of the N-Methyl-2-pyrrolidone (NMP) solvent in the matrix with the water in the coagulation bath, which promoted the phase separation. The structural parameter of the modified sub-layer containing 3.0 wt% PFSA decreased sharply to 334 µm from 1606.5 µm for pristine PVDF substrate, indicating reduced ICP effects and thereby, the water transport was increased. It can be seen a correlation between the hydrophilicity and water permeability. In RO filtration using DI water feed, the water permeability was rose monotonically to 2.79 LMH for 3.0 wt% PFSA incorporated membrane, however, it was declined for 5.0 wt%. PFSA incorporated membrane. When 10 mM NaCl was used during the experiment, the salt permeability was decreased to 0.39 LMH and the B/A ratio was lowered considerably to 12.84 kPa. The highest rejection value was of about 92.86 % and 92.23% for 5.0 and 3.0 wt%. PFSA incorporated membrane respectively.

Further improvement can be gained when disulfonated poly(arylene ether sulfone) incorporates PSf substrate. In addition to the sulfonic acid groups that improved the hydrophilicity, there was a good compatibility between both the hydrophobic and hydrophilic segments in the base polymer [148]. The optimal concentration was 25 wt.%, resulting in a higher water uphold capacity. The structure was more porous with narrow pore size and distribution, whilst the spongy structure provided the mechanical stability needed for large-scale experiments. Alongside, the structural parameter was lowered to 397 µm versus 1011 for a pristine membrane. These positive

changes provided satisfactory salt rejection results but lower water permeation. Unfortunately, the pure water permeability decreased dramatically when high loading of 25 wt% of BPSH100-BPS0 incorporated into the PSf polymer. The A was dropped to 1.57 LMH while B values was stable of 0.32 LMH for all membranes in RO test using DI water and 20 mM NaCl feeds. It was observed that a slight reduction in salt rejection by only 0.5%. It is worth noting that the pure water permeation for 3.0 wt.% PFSA embedded PVDF membrane outperformed the best results for the above additives. In terms of salt rejection, all the membranes achieved salt rejection over 90% and the highest value was for 25 wt% BPSH100-BPS0 embedded membrane.

A further development was to deposit a resin (IER-Na) into the PSf sub-layer during the preparation [159]. It is made of highly charged hydrophilic cross-linked polymer chains. Notably, these charges cause an electric repulsion on the outer surface to eliminate agglomeration of particles. Also, they provide charges on the pores in the inner surface. In comparison with a pristine membrane, the structural parameter decreased by 41.9% (1.62 ×10−4m)for 5 wt% IER-Na sub-layer and 1.74 ×10−4 m for 10 wt% IER-Na sub-layer. At concentration of 10 wt% IER-Na, there was a significant rise in water permeance by the double (4.08× 103 LMH) and the salt passage sharply increased to 13.36×104 LMH. The salt rejection remained stable at 96% as compared to a pristine membrane. At this optimum content, the water flow was better due to the formation of more passageway and charged pores. Likely, the water permeability of the developed membrane containing 10 wt% IER-Na was the highest of about 4.32 LMH but the salt permeability became high of 0.3778 LMH as compared to pristine membrane (A = 2.19 LMH and B= 0.0335 LMH). In FO process, the reduction of water flux was lower than that for for a membrane free of IER due to lower S value. Another research effort suggested the addition of either inorganic fillers or carbon molecular sieves into the base polymers due to providehigh transport rate.

6.5 Incorporating hydrophilic Nanomaterials

Currently, nanomaterial is the key technology for developing a new type of FO membranes. Nanocomposite membranes include several important features, such as enhanced mechanical properties, good adsorption capacity, and excellent rejection rate as well as chemical and thermal stability [160]. The homogenous dissolution of nanomaterials in the polymer matrix may raise the fractional free volume in mixed matrix membranes leading to high water permeability [161]. Nanotube materials can be described as additional water channels in the sub-layer. For example, CNT embedded polymeric membrane facilitated a fast flow of molecules estimated by 4-5 fold through the membrane due to smooth CNT walls [162]. It should consider the compatibility between the base polymer and the inorganic additive.The hydrophilicity of PSf membranes embedded graphene oxide (GO) was enhanced which can be ascribed to the abundant oxygen linked to the functional groups [163].

Systematic studies of two different types of graphene material presented comparable results based on the hydrophilicity, the structural parameter (S) and the membrane performance. For instance, Park et al [39] modified TFC-FO membrane using GO nanosheets. He reported a reduction in the structural parameter approaching 191 mm and a low tortuosity (τ). It was explained that it was caused by the hydroxyl, carboxyl and epoxy functional groups in GO, causing an increase in the membrane hydrophilicity. The pure water permeation was consistence with higher loading of GO nanosheets into the PSf polymer. A 0.25 wt.% concentration of GO shortened the mass diffusion of the salt leading to enhanced water permeability of about 1.76 LMH against pristine membrane (0.91 LMH). When 1000 mgL^{-1} NaCl FS was used in RO filtration, the rejection efficiency was also enhanced to 98.7% due to a low salt permeability coefficient (B)/ water

permeability coefficient (A) value of 0.11 bar and decreased ICP. Despite that, there was a serious decline in the water permeation at high loading of GO nanosheets such as 0.5%.wt and 1%.wt. Fouling caused by salt precipitation over the membrane surface was notable.

In comparison, when reduced graphene oxide based graphitic carbon nitride (CN/rGO) was used, a low selectivity ratio (A/B) was obtained [164]. It was attained because of high tortuosity of the pores and the agglomeration in the substrate that caused certain defects in the active layer. This might have occurred because a few of flakes in the PES support induced the formation of pores yielding a thicker substrate and increased porosity. High structural parameter of 463 μm was reported at 0.5 wt.% content of CN/rGO while it was lower of 163 μm for sub-layer containing 0.5%.wt CN/rGO. On the other hand, this structure benefited the water flux transport as it sharply approached 41.4 LMH. This result is higher than the pristine membrane by 20% against DI water and 2 M NaCl. This was due to its special structure consisting of curved nanosheets with a lamellar morphology that improved hydrophilicity. From the FO experimental results, the A, B, and S parameters were calculated. The water permeability sharply approached 2.99 LMH. This result is higher than that for the pristine membrane by almost 2 folds. Conversely, the undesired salt passage got higher of about 0.673 LMH. The salt rejection was almost steady using DI water FS and 0.5M NaCl DS in the FO system.

A further research by Morales-Torres et al [165] is to investigate the influence of different concentrations of multi-walled carbon nanotubes (MWNTS), functionalized MWCNTs (MWf) and graphene oxide (GO) in a PSf support layer. The impact of their physicochemical properties on surface chemistry and morphology and the effect of adding PVA or carbon-TiO_2 composites on the membrane properties were explored. The results revealed that the structures varied: the hydrophilic nanomaterials formed a macrovoid structure whilst the hydrophilic GO incorporated

MW formed finger-like macrovoids. The surface chemical properties of the nanomaterials enhanced the hydrophilicity of the PSf substrates. The greatest hydrophilicity was witnessed for membrane contained PVP and carbon-TiO_2 composites (GOT or MWfT) which had high substrate wettability and porosity, finger-like macrovoids and minimal ICP effects. The resultant membranes were evaluated in only FO experiment using DI water feed and a 0.6 M NaCl DS.

It exhibited a high water flux of 9.6-12.5 LMH versus a commercial TFC membrane using DI water feed and a 0.6 M NaCl DS. The membrane-based 0.5M WfT/M-P and PVA represented low solute reverse diffusion.

Moreover, it was reported in a recent paper that incorporating Alumina-Silicates (HNTs) in the PSf/TFC substrate influenced the morphology and membrane performance efficiency [18]. It was observed high porosity of 79%, large pores were created and the formation of channels facilitated the free flow of water flux through the membrane. There was a decrease in the structural parameter from 0.37mm to 0.95 mm. The hydrophilicity improved considerably due to the transfer of the fillers to the boundary layer, causing lower energy at the membrane interface. An ideal concentration of 0.5 wt.% (HNTs) of the new support layer achieved high pure water permeation of 2.0 LMH and high salt permeability of 9.34 $\times 10^{-8}$ m/s using DI and 20 mM NaCl in RO system. The salt rejection was lower of about 93% than that for pristine membrane (96%). It was found out that the high loading of HNTs influenced the cross-linking degree of PA suggesting reduced salt separation of about 81%. Thus, the salt permeability was increased when high content of HNTs was deposited into the sub-layer resulting in high B/A ratio of about 16.8 kPa.

Recently, a new PES substrate was developed by impregnating Zn_2GeO_4 nanowires. The hydrophilicity was barely enhanced and the sub-layer became thinner [166]. The hydrophilicity was little enhanced and the sub-layer became thinner [166]. There was a significant improvement in water permeability by ~ 45%; in contrast, salt rejection was retained in RO test using 2000 ppm

NaCl FS Unfortunately, this type of material is not sufficient in reducing the ICP effect and therefore water flux was declined using DI water FS and 0.5-2 NaCl DS in FO mode. An alternative is inorganic nanoparticles which can be used to promote the hydrophilicity, durability, thermal stability, water permeation and the salt rejection of TFC-FO membrane [40].

6.6 Incorporating hydrophilic Nanoparticles

Nanoparticles (NPs) have a central role in improving the physicochemical properties of the support layer as reported by several groups [116, 167,168]. The membrane characteristics can be influenced by poor dispersion of inorganic nanomaterials in the polymeric matrix or incompatibility with the polymeric membrane. It is expected that the very small size of nanoparticles is useful to make thinner membranes [161]. NPs can also induce the formation of a preferable finger-like structure with low tortuosity [116]. Also, it was witnessed that incorporating hydrophilic nanoparticles with a high surface area could hinder the thermodynamic stability. Thus, a fast exchange rate between the solvent and non-solvent might occur at the time of phase inversion [116]. Keeping this in view, the aim of depositing nanoparticles into polymeric membranes is to promote the hydrophilicity, mechanical strength, the water flux and separation property [169]. These studies focused on the improvement of hydrophilicity and morphology through various types of novel nanoparticles including Titanium dioxide grafted poly(2-hydroxyethyl methacrylate (TiO_2-g-PHEMA), Zeolite, Calcium Carbonate ($CaCO_3$) and silica. For example, the addition of Zinc oxide-Silicon dioxide, ZnO-SiO_2 (ZSCSNPs), impregnated in PES polymer suspension, enhanced the hydrophilicity and the morphology of its substrate [116]. Importantly, a sponge-like structure was formed and the structural parameter was declined from 723 to 271 μm. This is likely contributed to the significant increase in the water permeability. When DI water and 1000 ppm NaCl feeds were used in the RO experiment, the water permeability

was increased at high concentrations of (2%.wt ZSCSNPs) nanoadditives achieving 3.83 LMH, whilst the salt separation was poor of 72.43%. This indicated high salt permeability reaching 6.19 LMH versus 1.62 LMH for a pristine membrane.

Conventional nanoparticles such as Zeolite and titania showed acceptable water permeability and salt leakage due to a tailored sub-layer structure. Firstly, 0.5-1 wt.% porous zeolite nanoparticles embedded in a PSf support layer showed high porosity and the wettability while the substrate became thinner [15]. The resulting structure parameter was reduced to 0.34 mm from 0.96 mm for the pristine TFC membrane. However, when 0-0.9 wt.% content of hydrophilic titania nanoparticles with a size of <21 nm [167] was deposited into the PSf sub-layer, improvements were reported: good wettability, the formation of finger-like structures, low S value of 0.39 mm, reduced tortuosity and low ICP impacts. All these promising alterations in the sub-layer morphology contributed to good water permeability of 3.30 LMH and 4.27LMH for membranes containing 0.5 and 1.0 %.wt zeolite when using DI water feed in RO filtration. Furthermore, when 10 mM NaCl solution was used, the salt rejection was declined around~86% for membrane containing 1 wt% zeolite due to zeolite aggregation that affected the integrity of the selective layer.

Compared to the conventional nanoparticles, novel TiO_2-g-PHEMA was embedded into the PSf sub-layer [168]. The morphology of the sub-layer contained a spongy structure and finger-like structure because of delayed de-mixing during the phase inversion at high NPs concentration (3 wt.%). It was highlighted a sharp reduction in the structural parameter from 1347µm to 531µm for 3 wt.% NPs impregnated membrane. A significant increase in the water permeability was recorded of 2.41 LMH whereas the salt rejection was dropped to 88.1%. In comparison, a pristine membrane showed 0.99 LMH, 94.3% when using DI water and 10 mM NaCl feeds respectively in

RO system. Moreover, the B/A ratio was the highest of about 74.6 for membrane including 3%.wt content of NPs. It was decreased probably due to agglomeration of NPs on the upper surface of the substrate which may produce implications on the selective layer. It appeared that the double structure of the developed membrane showed higher water flux than that for membranes made only of a finger-like structure, which is in good agreement with Tiraferri et al [56].

Kuang et al [170] investigated the deposition of sacrificial Calcium Carbonate ($CaCO_3$) nanoparticles followed by hydrochloric acid (HCl) etching to increase the porosity. Attainment of interconnected pores and more porous structure can enhance the water flux of the newly developed membranes. It was observed a highly porous sub-layer and longer finger-like macrovoids that contributed to a smaller structural parameter (S=796 μm) and reduced ICP effects. Notably, the high water flux was estimated by 6.79 LMH and 9.31 LMH for membranes including 1:3 and 1:2 $CaCO_3$/ PSf ratio against a pristine membrane (4.07 LMH). At 2:3 $CaCO_3$/PSf ratio, the fabricated membrane possessed the water flux achieved the highest value of 14.2in RO test using 10 mM NaCl feed. However, the salt rejection was decline dramatically at higher NPs content reaching 81.7% at 10 wt.% NPs content. It can be attributed to the presence of defects and rougher selective layer arising from nanoparticle clusters. This may also affect the selective layer development.

Lu et al [171] recommended blending Mg and Al NPs, layered double hydroxide nanoparticles (LDH-NPs), into PSf polymer. At a high concentration of well dispersed NPs, a double increase in the porosity was observed. The difference with the earlier work was that a needle-like structure on the uppermost surface and spongy structure in the lower surface were formed. Thus, lower S value and thickness, as well as excellent wettability, allowed fast solute mass transfer in the sub-layer. The A, B and S intrinsic parameters were quantified by an Excel-based algorithm that described in section 2. At an optimal concentration of 2 wt.% NPs, the water permeability was

enhanced showing 0.61 LMH versus 0.48 for a pristine membrane using DI water feed and 1 M NaCl in FO test. The salt permeability was retained yielding a little change in A/B ratio corresponding 2.24.

In addition to the above research, amorphous silica nanoparticles, having a tiny size and high active surface area, were embedded into a nanofibrous PVDF substrate [172]. Due to the very small size of NPs, the were well dispersed, allowing good spinning of the resultant nanofibrous substrate. The viscosity of the dope solution was improved at higher NPs content, providing uniform dispersion and a higher diameter of the resultant fibres. Despite that, at 0.5% NP, the fibres mean diameter was reduced by 47% while a small structural parameter (S = 29.7 μm) and low tortuosity were reported. As shown in Fig.8, the transport of salt ions was low due to low S and τ values and mass transport resistance. Also, a high interfacial salt concentration caused a great osmotic driving force. This, in turn, improved the transport of water molecules within the sub-layer to the selective layer leading to increased water flux and vice versa. In this study, the algorithm procedure was also adapted to estimate the A and B values. It was suggested that the optimal amount of silica NPs was 0.5 wt % in TFC membranes to obtain the greatest salt rejection and water permeability. Subsequently, the water permeability achieved 1.36 LMH and the salt passage was decreased of about 0.884 LMH. The maximum salt rejection approached 99.7% in the FO process versus DI water FS and 2 M NaCl DS. Besides the modification of the sub-layer composition and morphology, the chemical treatment on the sub-layer surface may contribute to further enhancement in the water permeation and salt separation.

7 Advanced chemical modifications of the substrate

Several modification procedures have also been used to improve the FO membrane properties. The chemical modification involves the addition of a chemical modifier which adheres strongly to the surface by the covalent bonding providing chemical stability [173]. One of its advantages is providing low severe effects of ICP in the support layer and improving the water permeation [16]. For example, the separation properties of TFC-FO membranes can be affected by the physicochemical properties and microstructure of the porous support layer that are produced between the organic and aqueous phases during interfacial polymerization. This, in turn, can control the rejection tendency and the overall membrane performance [157]. High hydrophilicity arising from chemical modification may reduce the effect of membrane fouling, leading to the water permeation being improved considerably [119, 174, 175]. To date, there is a wide range of membrane modification methods documented in literature [176, 177] such as carbon nanotubes [178, 179], antibacterial nanoparticles like silver deposited in the substrate [180, 181] or coated on the TFC surface [182], grafting methods [175, 183], anionic coating to prevent the adhesion of organic foulants [182], hydrophilic polymer coating [184, 185] and zwitterionic coating [186, 187]. This section highlights the novel chemical modifications that were performed on various substrates of TFC-FO membranes involving a discussion on the pros and cons of each method and a comparison on the membrane productivity.

7.1 Chemical cross-linking treatment

It is acknowledged that grafting can be also used to improve the surface hydrophilicity of FO membranes. There are two different types of grafting: grafting describes the strong adherence of the chains in a solution to the surface whereas grafting from occurs when the polymer chains activate and are generated on the membrane surface [175].When the surface is negatively

charged, this will provide high separation of negative salt ions in the FS that are influenced by repulsion effects. For instance, Polybenzimidizole (PBI) is a potential material for FO membranes in the FO process [83]. Although it has good chemical resistance, high thermal and mechanical stabilities, a high ratio of surface area over unit module volume, is easy to scale up, inexpensive, has a high polarity and high water recovery and nanofiltration properties [62, 129], it suffers from quite low hydrophilicity and negative charges at neutral pH value [188].

Hausman et al [188] treated FO-PBI substrate, utilizing three modifiers (taurine, para-phenylene diamine, and ethylene diamine) and then the surface was initiated via 4-(chloromethyl) benzoic acid (CMBA) and N-ethyl-N(3-dimethylamino). The last step was carbodiimide (EDC) catalysis onthe final surface. This method was selected fora negatively charged sub-layer because it is hydrophobic, has no negative charges at neutral pH value, and there is a lack of effective wetting. The results revealed that treated PBI substrate became negatively charged and was transformed to hydrophilic due to the effective functionalizing by the three modifiers. Even though the water permeability was dropped significantly by 70% after this chemical modification, the monovalent salt separation was higher than that for the unmodified membrane. The reason behind this is that the negatively charged surface contributed to high salt rejection. The ultrafiltration test was undertaken utilizing NaCl feed with concentrations of 3.4 mM, 10mM, 20mM, 35mM, 100 mM and at pH = 7 and 10. However, there was a dramatic decline in the salt separation when the salt concentration was increased. To our knowledge, the swelling and high sulfonation degree issues in the sPSf can be counteracted by dispersing Polyethylene glycol (PEG) into sPSf polymer. Next, the resultant solution was applied to the PES/sPSf substrate [19]. The predominant function of this treatment is promoting the hydrophilicity and inhibiting fouling arising from the excessive ether oxygen groups in PEG. This cross-linker induced the adherence of the sub-layer to the selective layer. It was noted that this coating appeared uniform and homogenous on the

substrate. There was no significant change in the structure as it contained a sponge-like structure and large macrovoids interconnected perfectly close to the fabric backing layer. The surface hydrophilicity was much declined with a contact angle of 15.5^{o}. This membrane performance was examined in FO mode utilizing DI water FS and 2 M NaCl DS. Although the FO water flux was improved (15.2 LMH), the salt flux was severe (65.9 gMH) in comparison to commercial HTI membrane (13 LMH, 10.5 gMH). The salt rejection was low around 55% for NaCl and around 96% for $MgCl_2$ when the membrane assessed in FO test using a 1 g/L NaCl or $MgCl_2$ FS and a 2 mol/L glucose DS. This can be ascribed to the high density of the PEG at the greater concentration and the formation of compacted selective layer.

7.2 Polydopamine (PDA) based hydrophilic coatings

Generally, the hydrophobicity of the support layer encourages the formation of ICP in FO membranes. It is challenging to improve the wetting properties of the porous sub-layer. It was assumed that polydopamine (PDA) treatment would enhance the hydrophilicity, wettability of the sub-layer pores, and reduce ICP and fouling propensity [189]. It is a bio-polymer which acts like an adhesive [190] and it changes the surface chemistry associated with enhancing the wetting characteristics [191]. This treatment involves applying PDA on the top surface of the sub-layer which was prepared from the interaction between dopamine-HCl and Tris-HCl buffer solution [189]. It had positive outcomes on the substrate, like producing a fine hydrophilic surface and inducing the hydrophilicity of the intrinsic pore walls, as well as causing low pore size and small pore size distribution for better development of the active layer leading to high selectivity. The PES support layer was amenable to polydopamine modification to increase the flux permeability and salt rejection rate. Arena et al [192] found out that the hydrophilicity and wettability of the

modified RO membranes were enhanced for the FO system. This was confirmed by high water permeates corresponding 4-6 folds increase compared to pristine RO membranes. Furthermore, it was used to modify the NF membrane because it can be coated as a thin layer on the sub-layer surface and it provides a great hydrophilicity without sacrificing water permeation [193]. In Han et al's [194] work, the PDA functionalization was carried out on the PSf before the interfacial polymerization which caused an improvement in hydrophilicity of inner pores associated with enhanced stability, small pore size distribution and fine surface. There was not a notable decrease in the structural parameter. The lowest value was 1.51 X 10^{-3} m after 1 hour of PDA treatment on the substrate. Therefore, the highest A value was 0.6 LMH and the B value was as low as 0.19 LMH after 1 hour of the PDA coating on the sub-layer when utilizing DI water and 200 ppm NaCl feeds in RO filtration. Since the PAD coating time was longer than 1 hour, the salt permeability was reduced drastically and hence the salt rejection reached 88% after 5 hours of the PDA coating.

Liu et al [135] synthesized a membrane consisting of a mesh fabric sandwiched between a PA film on the top and a PSf layer on the bottom. The PDA treatment was applied on the bottom surface of the new membrane. The contact angle was reduced from 82.2° to 37.4° for the bottom surface after a treatment time of six hours. This is because the PDA coating originated more phenolic hydroxyl and amine groups on the surface which induces the hydrophilicity. Nonetheless, the A, B and salt rejection values retained similar results at various coating time to unmodified membrane against 2000 ppm NaCl solution in the RO test. It is important to control the deposition time because the pore size shrinkage and low pore size distribution were observable after six hours. This caused low solute diffusion within the sub-layer and lowered the water permeability compared to pristine membrane. However, the modified substrate had a good antifouling property.

7.3 Surface-coating via Poly vinyl alcohol (PVA)

PVA surface coating has several merits, including the ability to retain water molecules, its availability in the market, it is inexpensive and has great chemical and physical stability, is hydrophilic, has antifouling properties and remarkable film-forming characteristics [195, 196]. It has been developed as a coating film on PSf/UF to fabricate NF membrane [195, 197] and has also been used to enhance the hydrophilicity of UF membranes and is an antifouling agent [198]. The aim of using this modifier was to obtain highly hydrophilic substrate leading to higher water permeation and salt separation. Saraf et al [131] employed PVA coating to the PSf support layer of commercial seawater/brackish water (SW/BW) RO membranes. To obtain high strength and less swelling behaviour of PVA in water, cross-linking agents such as 10%, 50% maleic acid (MA) and 10%, 50% glutaraldehyde (GA) were used for coating SW/BW membranes respectively. Clearly, both the modified membranes exhibited decreased contact angles compared to pristine membranes but membrane treated with PVA-50% glutaraldehyde was hydrophobic. Opposite results were produced for membrane performance during RO experiments using 2000 ppm NaCl and FO test using DI water FS and various concentrations of NaCl. SW membranes treated PVA and 10% maleic acid achieved impressive water flux approximately 55 LMH than that for membranes treated with 50% PVA bounded GA. In spite of that, the modified BW30 membranes showed poor water flux approximately 5 LMH due to pore blockage by a PVA-50% glutaraldehyde agent. This hindered the flow of PVA into the bottom substrate of BW membranes to obtain the required hydrophilicity and it had a lower fractional free volume when highly cross-linked. Evidently, the reverse salt flux was very low because of pore clogging.

It is worth noting that the reaction time of the cross-linking agent could impact the porosity and pore size distribution of the membrane. It was suggested that GA as a cross-linker stabilized PVA on the membranes [199]. Conversely, the pore size distribution of the membrane could be reduced (or pore blockage) when the cross-linking reaction period was higher, arising from the interaction between hydroxyl groups in the PVA with the aldehyde groups of GA which formed a strong network structure in the PVA.As the reaction occurred between PVA and MA, free water molecular and ester were produced. In the end, some unbounded hydroxyl groups with PVA, water and ester introduced hydrophilicity to the PVA. In contrast, when PVA reacts with GA, an acetal was produced that contained low amounts of hydroxyl groups and became more hydrophobic [20]. It is likely a higher reaction time of PDA coating could create a thicker layer. Consequently, this raises the possibility of decreasing the mean pore size which influences the water permeation through the sub-layer.

7.4 Mineral ($CaCO_3$)-coated PES substrate

An alternative hydrophilization procedure is the bio-mineral coating of $CaCO_3$ on the PES substrate to improve wettability, which decreases the S value and ICP effects in TFC-FO membrane [200]. This coating was used for other polymeric membranes in previous studies [14, 201, 202]. It can provide the substrate with the required hydrophilicity because it can be connected to water through strong ionic hydrogen bonding. A PES sub-layer was exposed to bio-mineral ($CaCO_3$) coating to cover the inner surface of this layer [200]. In Fig. 9(a), the three stages for the preparation of the mineral coating are described. First, the polyacrylic acid (PAA) deposited into PES polymer to provide the negative charges. Then, PI was formed on the top surface followed by the mineral coating on the inner surface substrate. The PES/PAA5 appeared rough after the

alternative immersion procedure which indicated effective $CaCO_3$ coating as can be seen in Fig.9 (b). This coating enabled an effective hydrophilicity via the electrostatic interaction. This means the interaction between Ca^{2+} and carboxylate groups of PAA accelerated the nucleation of Ca^{2+} on the pore surface followed by an interaction with CO_3^{-2} to form the coating on the substrate [200, 14]. Additionally, the mineral coating contributed to a little decline in the water permeability when using DI water in RO experiment. This decrease caused by the swelling issue of PAA leading to contraction and pore blocking. However, it was useful in removing the PAA chains, resulting in larger space for water flux transport. Consequently, the transfer of water and solute flux were augmented through the membrane. Amongst all the modifications methods, this strategy produced the smallest S value of about 35.7 µm. Besides, the ICP effect was also decreased. The deposition of 5 vol% PAA in the coating resulted in a sufficient water flux of 52 LMH and salt flux of 16.8 gMH using DI water and 2 M NaCl DS in FO mode. The selectivity ratio (Js/Jw) was as low as 0.3 which indicated a good salt rejection (over 90%) against 200 ppm NaCl in RO test. It was also reported that the water permeability was comparable.

As such, this treatment provided the needed hydrophilicity for the substrate at a certain concentration was easy to prepare and was inexpensive [14]. The swelling of PAA was prevented by the addition of $CaCO_3$ which induced the disintegration of the PAA chains [202]. Optimizing the concentration of the PAA in the coating is important because its molecules can be released at a high concentration. Thus, the hydrophilicity might be retained, causing insufficient treatment to the substrate. The negative effect of depositing PAA in the coating was a lower mechanical strength of the developed membrane.

7.5 Application of aquaporin in the modification of FO membrane

Currently, the water channel protein aquaporin is used in fabricating FO membrane to facilitate water transport through the membrane [13]. A wide range of research has been carried out using different procedures to form aquaporin incorporated membranes [13, 90, 203, 204, 205]. Scientists are interested in aquaporin due to its effective performance. This was attained with the preferential water transport within the channels and superior solute separation. Even though the bilayer structure is unstable, it contributes to a fast flow of water through the membrane. Wang et al [90] prepared aquaporinZ incorporated dual-skinned FO membranes, through two stages. Initially, a polycationethyleneimine (PEI) was deposited followed by a polyanion polystyrene sulfonate (PSS) layer on the basis of a hydrolyzedpolyacrylonitrile (H-PAN) sub-layer. This step was applied to both the bottom and top surfaces of the sub-layer to make two selective layers. Lastly, to produce AqpZ-embedded SLB, 1,2-dioleloyl-sn-glycero-3-phosphocholine (DOPC) and 1,2-dioleoyl-3-trimethylammo-nium-propane (chloride salt) (DOTAP), the mixture proteoliposomes solutions was coated over L-b-L top surface. The hydrophilicity was greatly improved as firstly, there are strong bonds between water molecules, acidic COO− and amine groups on the PSS-terminated double-skinned (T-PSS) substrate and secondly, the hydrophilic property of supported lipid bilayer (SLB). The substrate structure comprised of finger-like pores. The roughness and pore size were varied on the top and bottom surfaces which influenced the stability of the selective layer. AqpZ-embedded dual-skinned FO membrane containing protein-to-lipid weight ratio (P/L) of 1/50 displayed low ICP and excellent antifouling. Only the results of FO test utilizing DI water feed and 2 M MgCl2 DS reported in this study. An acceptable water flux of 13.2 LMH and salt leakage of 3.2 g/m^2 h were obtained using DI water feed and 2 M $MgCl_2$ DS in FO mode.

Additionally, a novel strategy was developed to form stable aquaporin based biomimetic membranes with excellent FO performance [206]. This strategy is described in Fig. 10, it involved applying PDA coating on the PSf substrate and the deposition of proteoliposomes and NHS

solution. This was followed by an amidation reaction to create covalent bonds between PDA layer and 1, 2-dioleoyl-sn-glycero-3 phosphoethanolamine (DOPE) on the substrate. These interactions produced a stable AqpZ-embedded SLB. Fig.10 (b) showed flat uniform surface and the SLB is very thin, around 4–5 nm. It was reported that the hydrophilicity was improved significantly due to the presence of hydroxyl catechol and amine groups of PDA coating and it became much higher after depositing a supported-lipid bilayer (SLB). High water permeability was achieved for AqpZ-containing proteoliposomes rather than liposomes because the latter has a low shrinkage rate. In comparison to the above research, AqpZ-DOPE/DOTAPSLB membrane displayed a good performance with a higher water flux of 23.1 LMH and slightly lower salt leakage of nearly 3.1 gMH under the same conditions because of fewer defects of SLB. In RO mode using 2000 ppm $MgCl_2$, it was revealed that the highest salt rejection was 90% for AqpZ-DOPE/DOTAP SLB and the lowest salt permeability of 1.76 LMH. The water permeability was augmented showing 6.3 LMH as compared to AqpZ-DOPE SLB (A= 5.64 LMH). It can be suggested that high S value of 981µm can affect the performance of this AqpZ-DOPE/DOTAPSLB membrane.

However, the bio-mimic membrane is fragile, especially when it is used under applied hydraulic pressure [204]. This becomes challenging to use it for assessing the membrane performance properties. Thus, it should be constructed and supported perfectly to provide mechanical strength, stability and to avoid deformation during the experiment. Another significant issue is that the high porosity of sub-layer and large vesicle pore size [90] may surpass the salt passage within the membrane and hinder its applicability for FO desalination. Ultimately, the fabricated membrane is not easy to scale up as it involves a complex preparation procedure.

8 Conclusion and outlooks

A wide range of strategies have been employed for tailoring FO sub-layers for FO system. Most of these modifications were used to promote the hydrophilicity, biocompatibility of the membrane structure, and effective functionality to enhance the FO membrane performance.

Permeability/selectivity trade-off impact, the ICP, the swelling of the modified polymer, and complex modification process are the critical constrains for FO membranes. ICP is the main drawback as it causes a decline in the membrane efficiency, raises the operating cost, and reduces the stability of FO membranes. It was difficult to totally eliminate the ICP, nevertheless, some studies successfully reduced its impact by decreasing the structural parameter of FO sub-layer. To the best of our knowledge, the S value was irrespective of the FS and DS characteristics and concentrations. Notably, different methods were used in a wide range of studies to measure the structural parameter which may cast doubt on the accuracy of the results. Hence, it would be better to characterize the sub-layer based on a standard methodology for long-term FO operations.

Bulk modifications are a simple approach and could be utilized to alter the properties of the support layer such as hydrophilicity, morphology, stability, and compatibility with the selective layer. When the synthetic polymer blended with nanoadditives, some restrictions were recognized during the preparation procedure. One of the obstacles is the swelling behaviour of the altered polymer aiding to increase the undesired thickness of the support layer. The low solubility of a hydrophilic nanomaterial embedded hydrophobic base polymer is another problem. The nanoparticles embedded in sub-layer exhibited aggregations due to reduced miscibility at

high concentrations. Sometimes releasing these nanoparticles to the interface might have occurred. All of these obstacles may have a serious impact on the water flux and salt separation for bench scale and long-term operations.

Afterward the focus was on improving the FO membrane performance by surface-coatings, grafting, incorporating aquaporinZ and other methods. Excellent findings were obtained from most of the researches, particularly substrate coatings with optimal concentrations on the support layer. In contrast, drawbacks were reported for some modification methods; questions still remain as to the long-term stability of these methods for FO membranes during large scale operations.

Urgent research is required to examine additional eco-friendly and inexpensive nanomaterials or nanofibers. It is important to study the mechanism of interaction between these nanomaterials or nanofibers with the base polymer. The thermodynamic stability and kinematic viscosity of the polymer suspensions are crucial in order to evaluate the phase inversion process. The influence of novel nanoadditives on the fabrication process and the pore structure of the sub-layer should be considered. It might be useful to deposit a porous material linked to the pores of the sub-layer in order to prevent ICP impact. It can also serve as nanochannels to enhance the water flux diffusion and salt separation through the sub-layer. A diverse range of support layers have been used for pressure driven membranes and it would be interesting to tailor and optimize them for FO membranes. Lastly, theoretical simulations, promoting other sub-layer characteristics, adjusting existing chemical modification methods, testing more chemical and physical modification procedures and optimization of the developed FO membranes might be more effective to further minimize ICP impacts. However, all these suggestions will need to be explored. By combining two treatment methods to improve membrane productivity, this could be a

potential research direction in the future. Ongoing researches to develop suitable FO membranes are still on the laboratory scale and are not prepared for industrial scale or commercialization.

Acknowledgements

The authors would like to thank the Royal Society for funding this work through Royal Society International Collaboration Award (IC160133) and for Qatar Foundation for funding the PhD student Wafa Ali Suwaileh.

Figure Captions

Figure.1: A schematic diagram of a commercial FO- TFC membrane. Reproduced with permission from [116]. Copyright 2017 Elsevier.

Figure.2: Showing the typical FO system which operates under osmotic pressure difference using seawater feed, NaCl draw solute and FO membrane. Adapted with permission from [127]. Copyright 2012 Elsevier.

Fig.3: The most important properties for selecting the ideal membrane for osmosis process.

Fig.4: (a) a schematic illustration of Layer by Layer process. Adapted with permission from [87]. Copyright 2011 American Chemical Society.

Figure.5: (a) schematic diagram of the preparation to make a membrane with vertical pores. (b,c,d) SEM micrographs of TFC membrane showing vertical pores having open structure in both sides of sub-layer creating spongy structure. Adapted with permission from Liang et al. [105]. Copyright 2017 Elsevier.

Figure.6-a, b, c, d: represents TFC membrane embedded polyacrylonitrile (PAN)/cellulose acetate (CA) blended nanofibers mat that synthesized in DMF at various weight ratios: (a) PAN/CA 2/8, (b) PAN/CA 5/5, (c) PAN/CA 8/2, (d) pure PAN.

(e-f) Cross-sectional SEM image of TFC membranes embedded nanofibrous PAN layer. Adapted with permission from Bui and McCutcheon [113]. Copyright 2012 American Chemical Society.

Figure.7-a: The synthesis process of carboxylated polysulfone (CPSF).

(b) A comparison between the pristine PSf and CPSf in terms of microstructure. It is shown a spongy-like structure in the CPSf support layer. Adapted with permission from [149]. Copyright 2013 Elsevier.

Fig.8: 3D illustration of salt mass transfer through the support layer toward the active layer. (A) Salt concentration gradient at high tortuosity, (B) salt concentration gradient at low tortuosity, (C) salt ions pass in the case of high tortuosity, and (D) salt ions pass in the case of low tortuosity. Adapted with permission from [172]. Copyright 2015 American Chemical Society.

Figure.9: (a) A schematic diagram demonstrating the synthesis procedure of $CaCO_3$-coated PES support layer of TFC-FO membrane. (b) Micrograph images showing the PES top surface (a-c). Adapted from Liu et al [200]. Copyright 2016 Nature/Scientific reports.

Figure.10: (a) A diagram presenting the modification procedure to form AqpZ-incorporated SLB forward osmosis (FO) membrane. The PSf substrate (gray) was treated with PDA and followed by the deposition of the amide bonded DOPE SLB (orange).

(b) SEM micrographs show the asymmetrical structure with flat surface of the modified support layer. The SLB filled the gaps on the PDA-coated PSf membrane successfully. Adapted with permission from [206]. Copyright 2015 The Royal Society of Chemistry.

List of figures

Graphical abstract

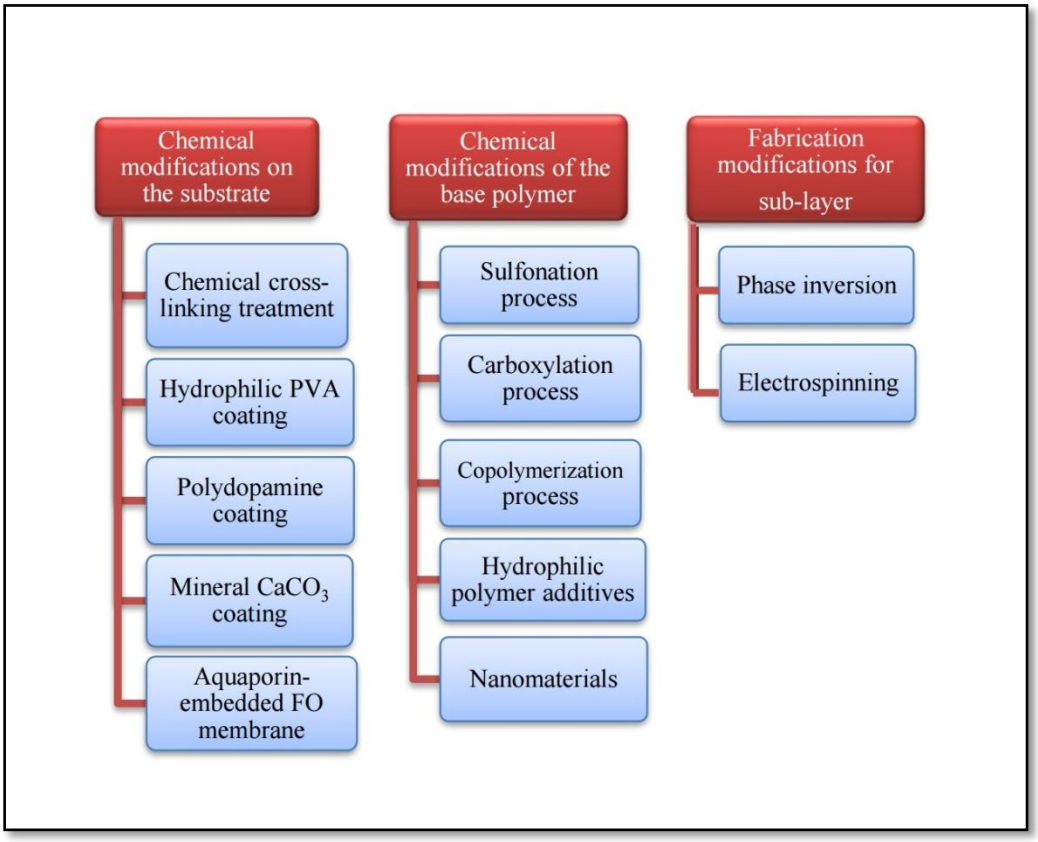

Figure.1

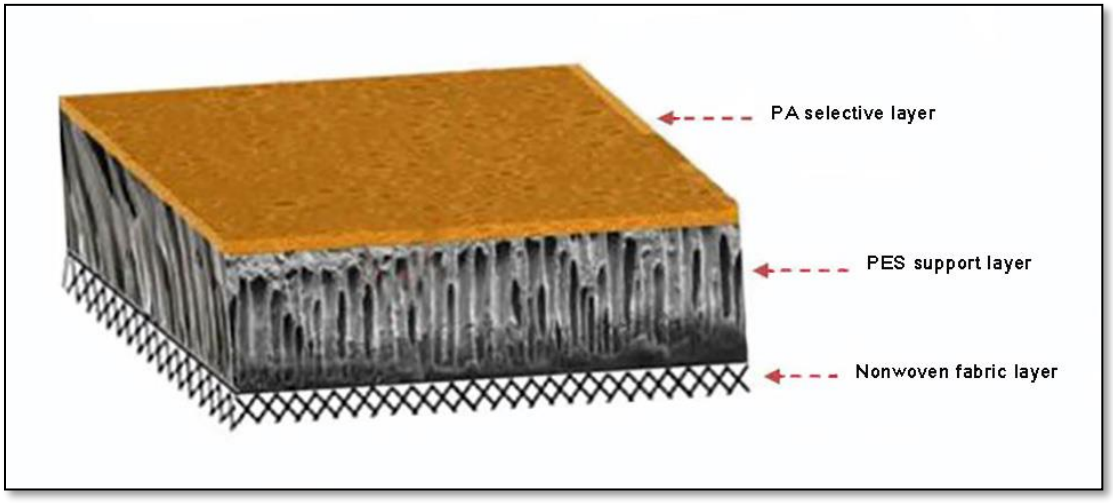

Figure.2

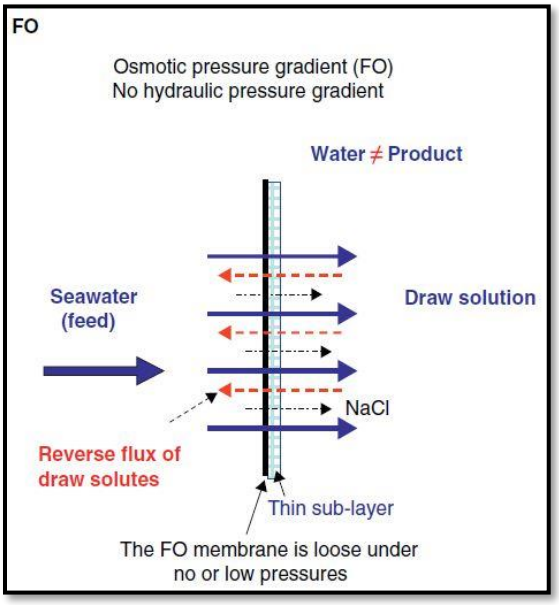

Figure.3:

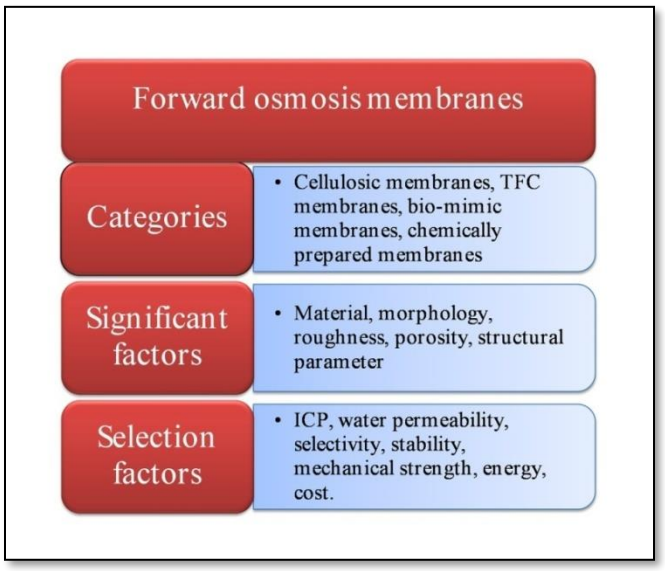

Figure.4

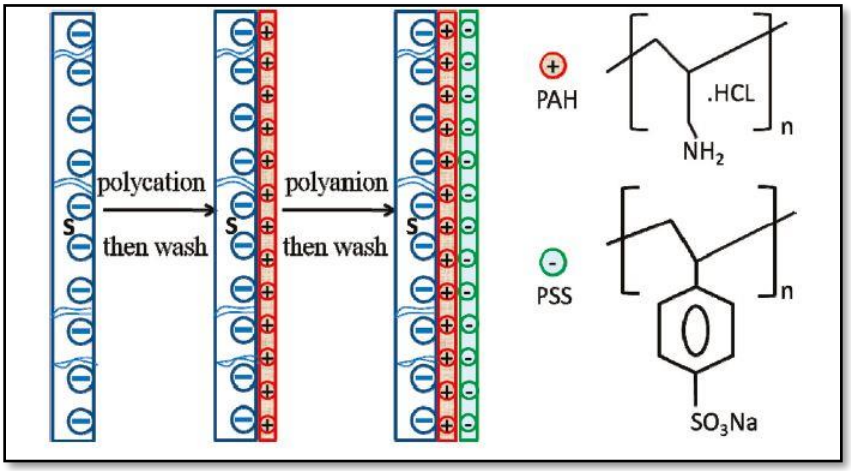

Figure.5-a

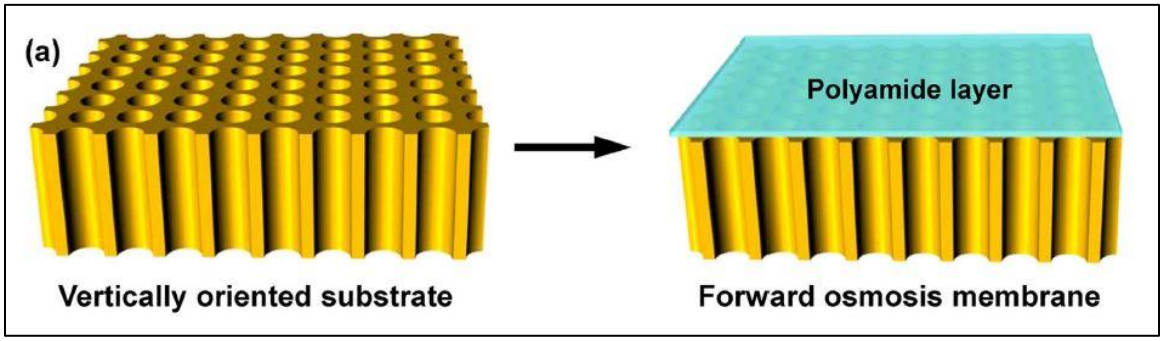

Figure.5-b

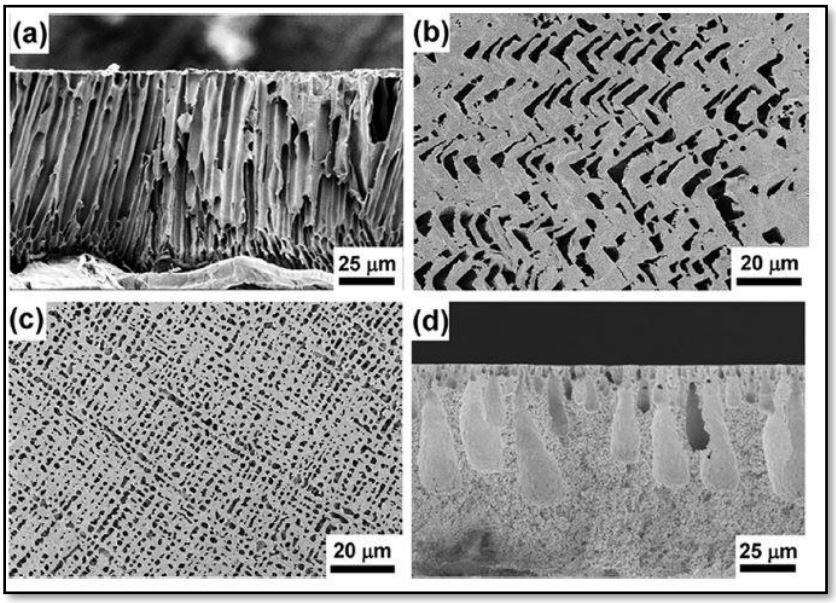

Figure.6

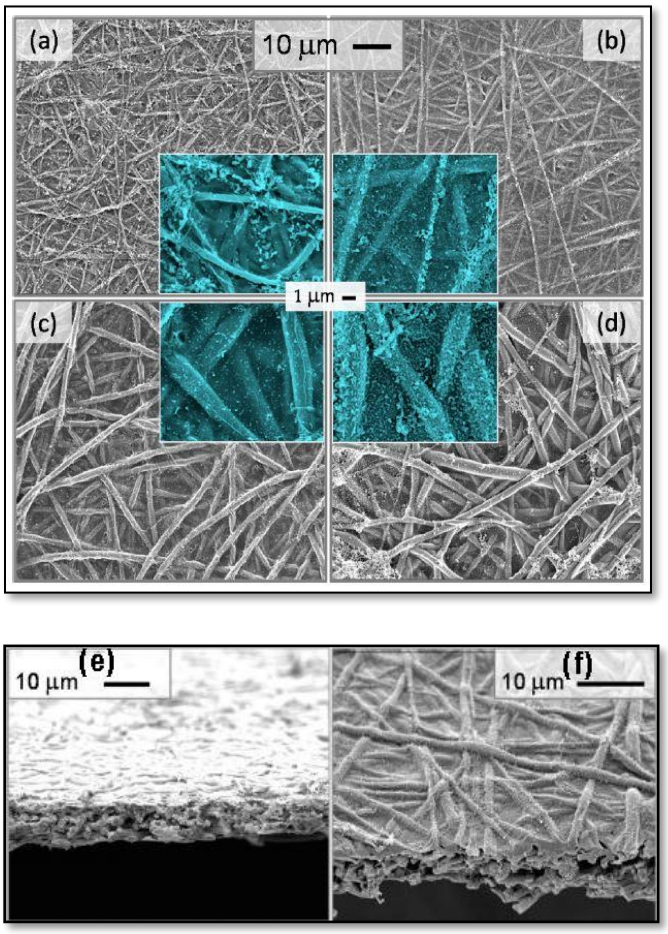

Figure.7-a

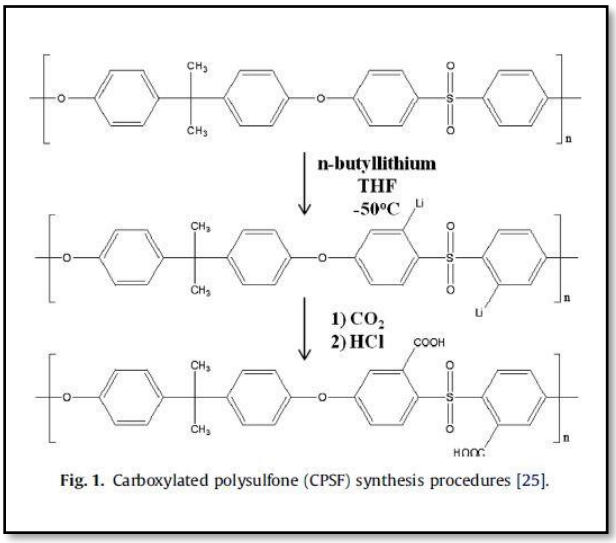

Fig. 1. Carboxylated polysulfone (CPSF) synthesis procedures [25].

Figure.7-b

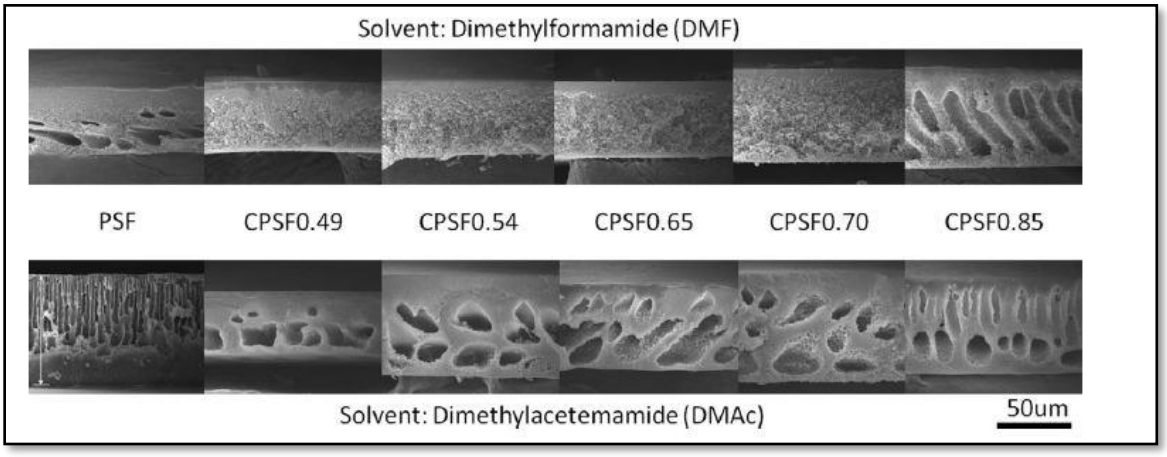

Figure.8

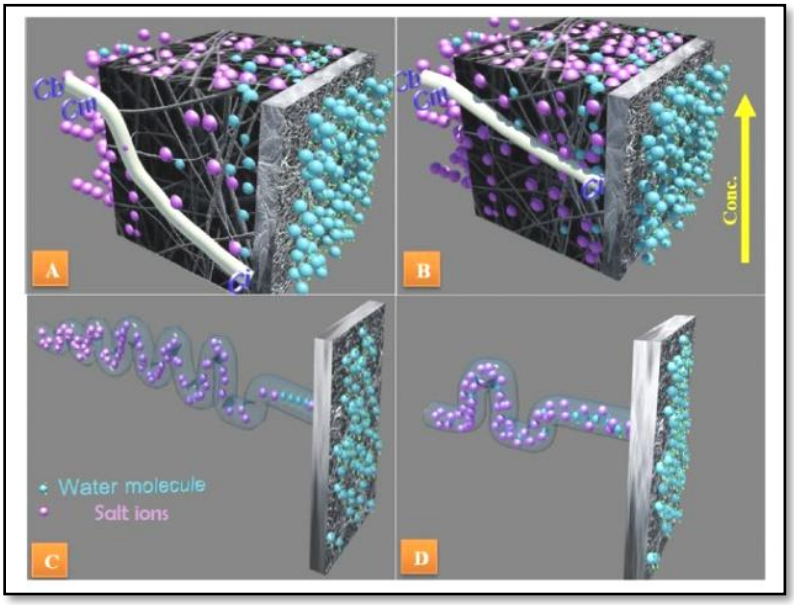

Figure.9-a

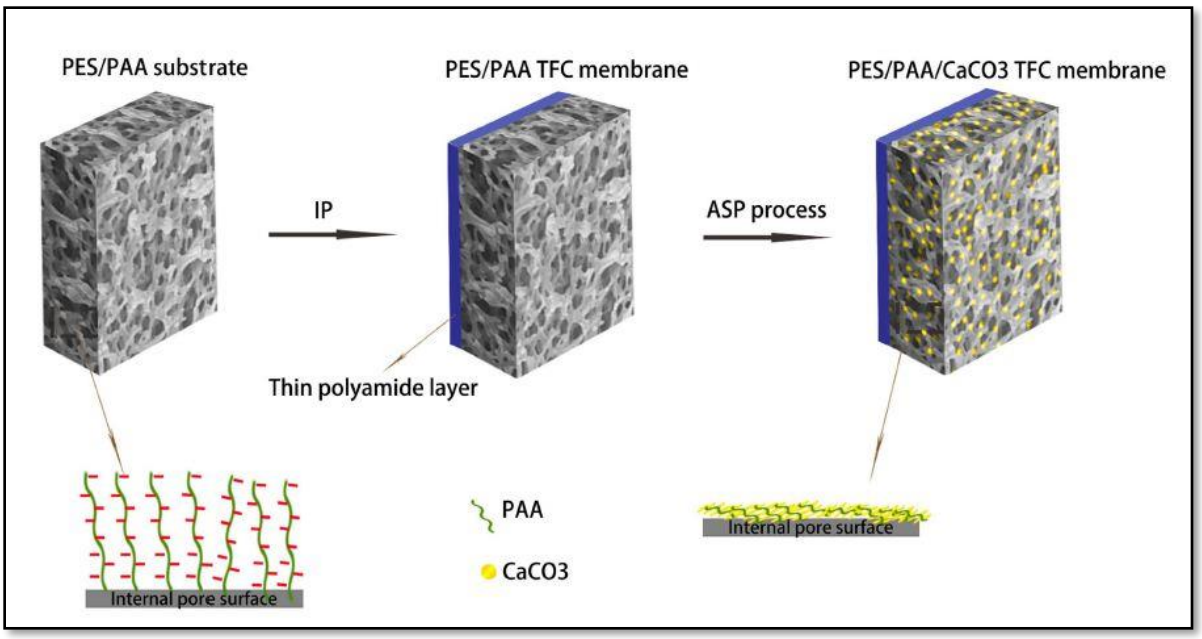
PES/PAA substrate
PES/PAA TFC membrane
PES/PAA/CaCO3 TFC membrane
IP
ASP process
Thin polyamide layer
Internal pore surface
PAA
CaCO3
Internal pore surface

Figure.9-b

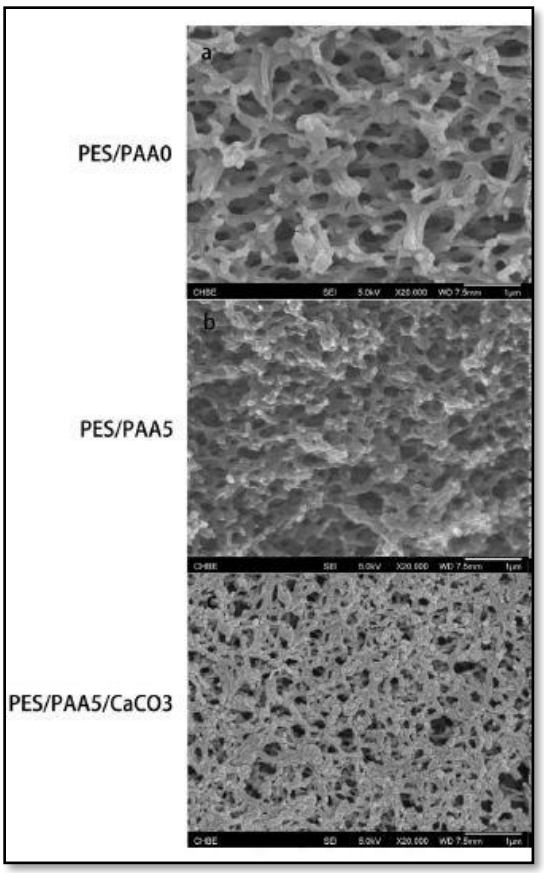

Figure.10-a

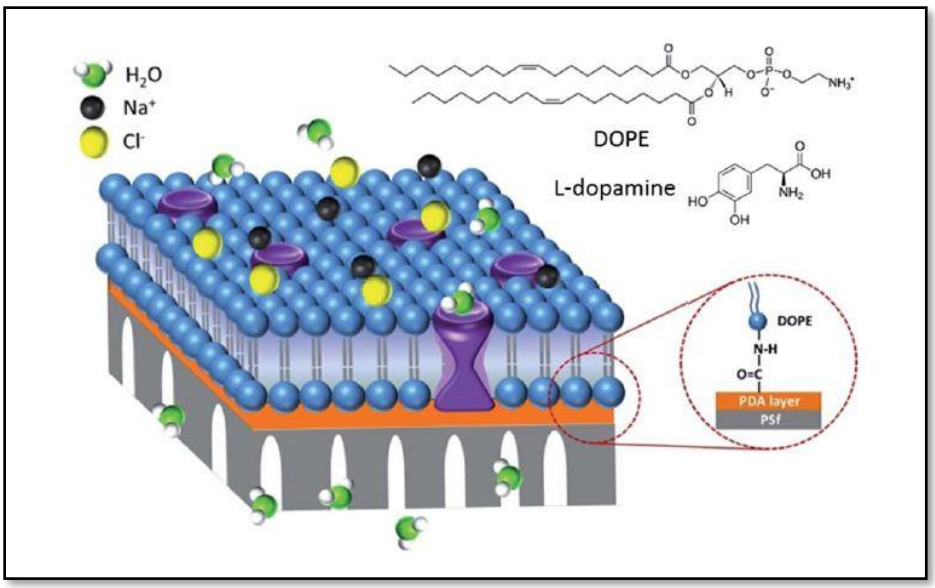

Figure.10-b

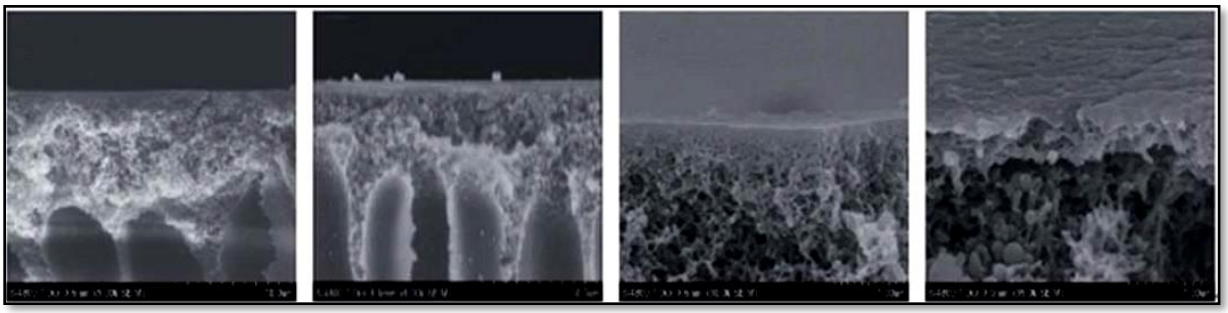

List of tables: Table.1: A diverse range of the FO membranes documented in earlier studies.

Year	Membrane category	Base materials	Fabrication method	Membrane function	Reference
2005	Capsule wall	Cellulose acetate (CA) or ethyl cellulose	Dip-coating, phase inversion	-	[62]
2006	HTI CA flat-sheet	Cellulose acetate (CA) Polyester mesh	Phase inversion	-	[10]
2006	HTI CTA flat-sheet	Cellulose triacetate Woven fabric mesh	Phase inversion	-	[207]
2007	NF hollow fibres	Polybenzimidazole (PBI)	Dry-jet wet spinning and interfacial polymerization (IP)	-	[62]
2009	Dual-layer NF hollow-fibres	polybenzimidazole-polyethersulfone (PBI-PES) Polyamide active layer	Dry-jet wet spinning blending with polyvinyl pyrrolidone (PVP) Interfacial polymerization (IP) for the selective layer	Protein enrichment	[208]
2010	TFC-hollow fibre with RO-like skin layer	PES Polyamide active layer	Support layer: dry–jet wet spinning process Selective layer: Interfacial polymerization (IP)	Wastewater treatment, water purification and seawater desalination.	[22]
2010	TFC flat sheet	PSf support layer Polyamide selective layer	Support layer: phase inversion Selective layer: Interfacial polymerization (IP)	Water and wastewater treatment, and power generation	[12]

2011	Double skinned TFC hollow fibre membranes with an RO-like selective skin and an NF-like secondary selective skin	Poly(amide–imide) (PAI) polymer Polyamide active layer	Phase inversion, IP chemical modification to form a polyamide RO like inner skin. PEI cross-linking to form positively charged NF-like outer skin.	Seawater desalination	[107]
2011	Nanfibrous PES-FO	PES nanofiber support layer Polyamide active layer	phase inversion, electrospinning Interfacial polymerization (IP)	Seawater desalination	[110]
2011	PA TFC flat sheet	Support layer: PESU-co-sPPSU 11 sulphonated PES polymer Polyamide active layer	Phase inversion Interfacial polymerization IP)	Water desalination/ power generation	[143]
2011	FO modified flat sheet membrane	Polyacrylonitrile (PAN) support layer	Layer by Layer (L b-L) assembly	Seawater desalination Power generation	[87]
2011	Hollow fibre with NF like skin	Poly(amide–imide) PAI	Non-solvent induced phase separation (NIPS) technique Chemical post-treatment with PEI cross-linking to form NF skin layer	Seawater desalination Power generation	[83]
2011	Nanoporous PES flat sheet	Polyamide active layer PES support layer PET nonwoven fabric	phase inversion	Wastewater desalination	[32]

2012	TFC-dual hollow fibres-NF skin	The fibre consists of two layers made from polyamide- imide (PAI) polymer for the outer layer and polyethersulfone (PES) polymer for the porous inner layer	Non-solvent induced phase inversion (NIPS) technique Chemical post-treatment with PEI cross-linking to form NF skin layer	Seawater desalination Power generation	[107]
2012	TFC hollow fibre	Polyethersulfone (PES) support layer	Dry-jet wet spinning process with advanced co-extrusion technology and IP	Seawater desalination Power generation	[209]
2013	TFC flat sheet	CTA support layer PSf support layer and polyamide active layer	Phase inversion Interfacial polymerization (IP)	Seawater desalination and Lysozyme (LYS) and alginate (ALG) removal	[210]
2013	TFC- multiwalled carbon nanotubes (MWCNTs) hollow fibers	Immobilizedpolyethylene imine–poly (amide–imide) (PAI)	Dry-jet wet spinning technique with Phase inversion chemical post-treatment using PEI	Seawater desalination	[211]
2013	Modified hollow fibres	Polybenzimidazole-polyethersulfone (PBI / Polyhedral Oligomeric Silsesquioxane nanoparticles (POSS) outer layer and a Polyacrylonitrile (PAN) inner layer	Dry-jet wet spinning technique Post treatment via thermal annealing	Water desalination/ power generation	[80]
2013	TFC (PSf/PA) flat sheet	Polyethylene terephthalate nanofibers backing layer Polysulfone (PSf) suppoer layer Polyamide active layer	Phase inversion Electrospinning Interfacial polymerization (IP)	Wastewater treatment Power generation	[123]

2013	TFC flat sheet	Polyvinylidene fluoride (PVDF) nanofibers support layer Polyamide active layer	Electrospinning Interfacial polymerization (IP)	Water desalination / energy production	[124]
2014	TFC flat sheet	PSf and sulfonated poly(phenylene oxide) support layer Polyamide active layer	Phase inversion Interfacial polymerization (IP)	Seawater desalination/ power generation	[212]
2014	TFC flat sheet	PVA nanofiber support layer Polyamide active layer	Electrospinning Chemical cross-linking via acid catalyzed glutaraldehyde	Water desalination	[213]
2014	TFN flat sheet	PSf support layer PA/silicon dioxide (SiO_2) active layer Polyester non-woven fabric backing layer	Phase inversion Interfacial polymerization (IP)	Seawater desalination	[214]
2014	TFN flat sheet	Polysulfone–titanium dioxide (PSf/TiO_2) support layer Polyamide active layer	Phase inversion Interfacial polymerization (IP)	Seawater desalination Power generation	[215]
2015	CTA hollow fibre	Cellulose triacetate (CTA) and outer polyamide (PA) active layer.	Phase inversion Dry-jet wet-spinning process	Seawater desalination Power generation	[216]
2015	TFC flat sheet	Multi-zoned nylon 6,6 MF support layer and nonwoven fabric backing layer Polyamide support layer	Interfacial polymerization (IP)	Seawater desalination Power generation	[217]

2015	Modified TFC flat sheet	Polysulfone (PSf) with PET mesh-embedded double skinned support layer and surface treated by polydopamine (PDA) Polyamide active layer	Phase inversion Interfacial polymerization (IP)	Seawater desalination power generation Alginate and silica separation	[135]
2016	TFC hollow fibre	Polysulfone support layer PA active layer	Dry-jet wet-spinning process with advanced coextrusion technology using a dual-layer spinneret Interfacial polymerization (IP)	Mass transfer modeling	[218]
2016	Modified CTA flat sheet	Cellulose triacetate (CTA) Carboxylic and amine functionalized carbon nanofiber CNFs (CNF-NH_2)	Phase inversion	Seawater desalination	[219]
2017	TFC flat sheet	Polyethylene terephthalate (PET) and Polyvinyl alcohol (PVA) nanofibers backing layer PVDF support layer Polyamide active layer	Electrospinning Phase inversion Interfacial polymerization (IP)	Seawater desalination	[220]
2017	TFC flat sheet	Polyketone polymer support layer PA active layer	Non-solvent induced phase inversion Interfacial polymerization (IP)	Seawater desalination	[221]
2017	Modified TFC flat sheet	Polysulfone (PSf) blended sodium type ion exchange resin (IER-Na) Polyamide active layer	Blending and wet-phase inversion IP	Water desalination Power generation	[159]

2017	Modified CTA flat sheet	Cellulose triacetate with binary mixed additives (acetic acid-lactic acid (AA-LA), acetic acid-maleic acid (AA-MA) as well as zinc chloride-lactic acid ($ZnCl_2$-LA)	Blending and non-solvent induced phase inversion	Seawater desalination	[222]

List of references

[1] R. McGinnis, M. Elimelech, Global challenges in energy and water supply: The promise of engineered osmosis, Environ. Sci. Technol, 42, (2008) 8625–8629.
[2] T. Y. Cath, N. T. Hancock, C. D. Lundin, Ch. Jones, J. E. Drewes, A multi-barrier osmotic dilution process for simultaneous desalination and purification of impaired water, Journal of Membrane Science, 362 (2010) 417– 426.
[3] A. Achilli, T. Y. Cath, A. E. Childress, Selection of inorganic-based DSs for forward osmosis applications, Journal of Membrane Science, 364 (2010) 233–241.
[4] K. Lutchmiah, A. R. D. Verliefde, K. Roest, L. C. Rietveld, E. R. Cornelissen, Forward osmosis for application in wastewater treatment: a review, Water research, 58 (2014) 179-197.
[5] T. Y. Cath, A. E. Childress, M. Elimelech, Forward osmosis: Principles, applications, and recent developments, Journal of Membrane Science, 281 (2006) 70–87.
[6] Y. Wang, K. Goh, X. Li, L. Setiawan, R. Wang, Membranes and processes for forward osmosis-based desalination: Recent advances and future prospects, Desalination (2017).
[7] R. McGinnis, G. McGllrgan, Forward osmosis membranes cross reference to related applications, Patent No.: US 8,181 (2012) 794 B2.

[8] K. L. Hickenbottom, N. T. Hancock, N. R. Hutchings, E. W. Appleton, E. G. Beaudry, P. XU, T. Y. Cath, Forward osmosis treatment of drilling mud and fracturing wastewater from oil and gas operations, Desalination, 312 (2013) 60–66.

[9] W. Ding, Y. Li, M. Bao, J. Zhang, C. Zhang, J. Lub, Highly permeable and stable forward osmosis (FO) membrane based on the incorporation of Al_2O_3 nanoparticles into both substrate and polyamide active layer, RSC Adv., 7 (2017) 40311–40320.

[10] J. R. McCutcheon, R. L. McGinnis, M. Elimelech, Desalination by ammonia–carbon dioxide forward osmosis: Influence of draw and FS concentrations on process performance, Journal of Membrane Science, 278 (2006) 114–123.

[11] N. Y. Yip, A. Tiraferri, W. A. Phillip, J. D. Schiffman, M. Elimelech, High performance thin-film composite forward osmosis membrane, Environ. Sci. Technol, 44 (2010) 3812–3818.

[12] F. Lotfi, L. Chekli, Sh. Phuntsho, S. Hong, J. Y. Choi, S. Hong, J. Y. Choi, H. K. Shon, Understanding the possible underlying mechanisms for low fouling tendency of the forward osmosis and pressure assisted osmosis processes, Desalination, (2017).

[13] Z. Li, R. V. Linares, S. Bucs, L. Fortunato, C. Hélix-Nielsen, J. S. Vrouwenvelder, N. Ghaffour, T. Leiknes, G. Amy, Aquaporin based biomimetic membrane in forward osmosis: chemical cleaning resistance and practical operation, Desalination, 420 (2017) 208–215.

[14] P. Chen, L. Wan, Z. Xu, Bio-inspired $CaCO_3$ coating for superhydrophilic hybrid membranes with high water permeability, J. Mater. Chem, 22 (2012) 22727.

[15] N. Ma, J. Wei, S. Qi, Y. Zhao, Y. Gao, Ch. Y. Tang, Nanocomposite substrates for controlling internal concentration polarization in forward osmosis membranes, Journal of Membrane Science, 441 (2013) 54–62.

[16] J. Ren, J. R. McCutcheon, A new commercial thin film composite membrane for forward osmosis, Desalination, 343 (2014) 187–193.

[17] N. Ma, J. Wei, R. Liao, Ch. Y. Tang, Zeolite-polyamide thin film nanocomposite membranes: Towards enhanced performance for forward osmosis, Journal of Membrane Science, 405– 406 (2012) 149–157.

[18] M. Ghanbari, D. Emadzadeh, W. J. Lau, H. Riazi, D. Almasi, A. F. Ismail, Minimizing structural parameter of thin film composite forward osmosis membranes using polysulfone/halloysite nanotubes as membrane substrates, Desalination, 377 (2016) 152–162.

[19] X. Ding, Z. Liu, M. Hua, T. Kang, X. Li, Y. Zhang, Poly(ethylene glycol) crosslinked sulfonated polysulfone composite membranes for forward osmosis, J. APPL. POLYM. SCI., 133 (2016) 39.

[20] B. D. Coday, B. G. M. Yaffe, P. Xu, T. Y. Cath, Rejection of trace organic compounds by forward osmosis membranes: A literature review, Environ. Sci. Technol, 48 (2014) 3612−3624.

[21] Q. Ge, M. Ling, T. Chung, Draw solutions for forward osmosis processes: Developments, challenges, and prospects for the future, Journal of Membrane Science, 442 (2013) 225-237.

[22] R. Wang, L. Shi, Ch. Y. Tang, Sh. Chou, Ch. Qiu, A. G. Fane, Characterization of novel forward osmosis hollow fiber membranes, Journal of Membrane Science, 355 (2010) 158–167.

[23] H. Tong, M. Wang, Electrospinning of fibrous polymer scaffolds using positive voltage or negative voltage: a comparative study, Biomed. Mater., 5 (2010) 054110.

[24] S. Kaur, S. Sundarrajan, D. Rana, T. Matsuura, S. Ramakrishna, Influence of electrospun fiber size on the separation efficiency of thin film nanofiltration composite membrane, Journal of Membrane Science, 392–393 (2012) 101–111.

[25] B. S. Lalia, V. Kochkodan, R. Hashaikeh, N. Hilal, A review on membrane fabrication: Structure, properties and performance relationship, Desalination, 326 (2013) 77–95.

[26] C. Feng, K.C. Khulbe, T. Matsuura, S. Tabe, A.F. Ismail, Preparation and characterization of electro-spun nanofiber membranes and their possible applications in water treatment, Separation and Purification Technology, 102 (2013) 118–135.

[27] P. Bertrand, A. Jonas, A. Laschewsky, R. Legras, Ultrathin polymer coatings by complexation of polyelectrolytes at interfaces: suitable materials, structure and properties, Macromol. Rapid Commun, 21 (2000) 319–348.

[28] M. L. Bruening, D. M. Dotzauer, P. Jain, L. Ouyang, G. L. Baker, Creation of functional membranes using polyelectrolyte multilayers and polymer brushes, Langmuir, 24 (2008) 7663-7673.

[29] J. Wei, X. Liu, Ch. Qiu, R. Wang, Ch. Y. Tang, Influence of monomer concentrations on the performance of polyamide-based thin film composite forward osmosis membranes, Journal of Membrane Science, 381 (2011) 110–117.

[30] Sh. Zhao, L. Zou, Ch. Y. Tang, D. Mulcahy, Recent developments in forward osmosis: Opportunities and challenges, Journal of Membrane Science, 396 (2012) 1–21.

[31] G. Li, X. Li, T. He, B. Jiang, C. Gao, Cellulose triacetate forward osmosis membranes: preparation and characterization, Desalination and Water Treatment, 51: 13-15 (2013) 2656-2665.

[32] Y. Yu, S. Seo, I. Kim, S. Lee, Nanoporous polyethersulfone (PES) membrane with enhanced flux applied in forward osmosis process, Journal of Membrane Science, 375 (2011) 63–68.

[33] X. Song , Z. Liu, D. D. Sun, Nano gives the answer: Breaking the bottleneck of internal concentration polarization with a nanofiber composite forward osmosis membrane for a high water production rate, Adv. Mater., 23 (2011) 3256–3260.

[34] I. Pinnau, B. D. Freeman, Formation and modification of polymeric membranes: overview, ACS SympSer, 744 (2000) 1–22.

[35] R. Guan, H. Zou, D. Lu, Ch. Gong, Y. Liu, Polyethersulfone sulfonated by chlorosulfonic acid and its membrane characteristics, European Polymer Journal, 41 (2005) 1554–1560.

[36] B. V. der Bruggen, Chemical modification of polyethersulfone nanofiltration membranes: a review, Journal of Applied Polymer Science, 114 (2009) 630–642.

[37] J. Ren, J. R. MucCutcheon, Polyacrylonitrile supported thin film composite hollow fiber membranes for forward osmosis, Desalination, 372 (2015) 67–74.

[38] V. Vatanpour, S. S. Madaeni, L. Rajabi, S. Zinadini, A. A. Derakhshan, Boehmite nanoparticles as a new nanofiller for preparation of antifouling mixed matrix membranes, Journal of Membrane Science, 401– 402 (2012) 132–143.

[39] M. J. Park, Sh. Phuntsho, T. He, G. M. Nisola, L. D. Tijing, X. Li, G. Chen, W. Chung, H. K. Shon, Graphene oxide incorporated polysulfone substrate for the fabrication of flat-sheet thin-film composite forward osmosis membranes, Journal of Membrane Science, 493 (2015) 496–507.

[40] X. Liu, H. Y. Ng, Fabrication of layered silica–polysulfone mixed matrix substrate membrane for enhancing performance of thin-film composite forward osmosis membrane, Journal of Membrane Science, 481 (2015) 148–163.

[41] M. Chwatko, J. T. Arena, J. R. McCutcheon, Norepinephrine modified thin film composite membranes for forward osmosis, Desalination, 423 (2017) 157–164.

[42] Q. Ge, M. Ling, T. Chung, Draw solutions for forward osmosis processes: Developments, challenges, and prospects for the future, Journal of Membrane Science, 442 (2013) 225–237.
[43] J. Qin, W. C. L. Lay, K. A. Kekre, Recent developments and future challenges of forward osmosis for desalination: a review, Desalination and Water Treatment, 00 (2012) 1–14.
[44] J. R McCutcheon, M. Elimelech, Modeling water flux in forward osmosis: Implications for improved membrane design, AIChE Journal, 53 (2007) 7.

[45] Forward Osmosis Tech's forward osmosis guide. http://www.forwardosmosistech.com/forward-osmosis-membranes/.

[46] L. F. Greenlee, D. F. Lawler, B. D. Freeman, B. Marrot, Ph. Mouling, Reverse osmosis desalination: Water sources, technology, and today's challenges, Water research, 43 (2009) 2317–2348.

[47] D. J. Johnson, W. A. Suwaileh, A. Mohammed, N. Hilal, Draw solutes for forward osmosis: a revolution in water treatment and desalination, Desalination, (2017).

[48] M. Qasim, N. A. Darwish, S. Sarp, N. Hilal, Water desalination by forward (direct) osmosis phenomenon: A comprehensive review, Desalination, 374 (2015) 47–69.

[49] B. Kim, G. Gwak, S. Hong, Review on methodology for determining forward osmosis (FO) membrane characteristics: Water permeability (A), solute permeability (B), and structural parameter (S), Desalination, 422 (2017) 5–16.

[50] Sh. Phuntsho, S. Sahebi, T. Majeed, F. Lotfi, J. E. Kim, H. K. Shon, Assessing the major factors affecting the performances of forward osmosis and its implications on the desalination process, Chemical Engineering Journal, 231 (2013) 484–496.

[51] B. Kim, G. Gwak, S. Hong, Review on methodology for determining forward osmosis (FO) membrane characteristics: Water permeability (A), solute permeability (B), and structural parameter (S), Desalination, 422 (2017) 5–16.

[52] A. Tiraferri, N. Y. Yip, A. P. Straub, S. R. Castrillon, M. Elimelech, A method for the simultaneous determination of transport and structural parameters of forward osmosis membranes, Journal of Membrane Science, 444 (2013) 523–538.

[53] Sh. Phuntsho, S. Vigneswaran , J. Kandasamy , S. Hong, S. Lee, H. K. Shon, Influence of temperature and temperature difference in the performance of forward osmosis desalination process, Journal of Membrane Science, 415–416 (2012) 734–744.

[54] J. R. McCutcheon, M. Elimelech, Influence of concentrative and dilutive internal concentration polarization on flux behavior in forward osmosis, Journal of Membrane Science, 284 (2006) 237–247.

[55] P. S. Singh, S. V. Joshi, J. J. Trivedi, C. V. Devmurari, A. P. Rao, P. K. Ghosh, Probing the structural variations of thin film composite RO membranes obtained by coating polyamide over polysulfone membranes of different pore dimensions, Journal of Membrane Science, 278 (2006) 19–25.

[56] A. Tiraferri, N. Y. Yip, W. A. Phillip, J. D. Schiffman, M. Elimelech, Relating performance of thin-film composite forward osmosis membranes to support layer formation and structure, Journal of Membrane Science, 367 (2011) 340–352.

[57] I. L. Alsvik, M. Hagg, Pressure Retarded Osmosis and Forward Osmosis Membranes: Materials and Methods, Polymers, 5 (2013) 303–327.

[58] S. S. S. Loeb, Sea water demineralization by means of an osmotic membrane, 38 (1963) 117–132.

[59] S. Zhang, K. Y. Wang, T. Chung, H. Chen, Y. C. Jean, G. Amy, Well-constructed cellulose acetate membranes for forward osmosis: Minimized internal concentration polarization with an ultra-thin selective layer, Journal of Membrane Science, 360 (2010) 522–535.

[60] R. E. Kravath, J. A. Davis, Desalination of sea water by direct osmosis, Desalination, 16 (1975) 151–155.

[61] K. Wang, Q. Yang, T. Chung, R. Rajagopalan, Enhanced forward osmosis from chemically modified polybenzimidazole (PBI) nanofiltration hollow fiber membranes with a thin wall, Chemical Engineering Science, 64 (2009) 1577–1584.

[62] K. Wang, T. Chung, J. Qin, Polybenzimidazole (PBI) nanofiltration hollow fiber membranes applied in forward osmosis process, Journal of Membrane Science, 300 (2007) 6–12.
[63] T. Chung, S. Zhang, K. Y. Wang, J. Su, M. M. Ling, Forward osmosis processes: Yesterday, today and tomorrow, Desalination, 287 (2012) 78–81.
[64] G. M. Geise, H. S. Lee, D. J. Miller, B. D. Freeman, J. E. McGrath, D. R. Paul, Water purification by membranes: The role of polymer science, J. Polym. Sci. B: Polym. Phys, 48 (2010) 1685–1718.

[65] J. Herron, asymmetric forward osmosis membranes, United States Patent: US 7445712B2, 2008.

[66] Ph. A. William, Y. Sh. Jui, E. Menachem, Reverse draw solute permeation in forward osmosis: Modeling and experiments, Environ. Sci. Technol., 44 (2010) 5170–5176.

[67] Ch. Y. Tang, Q. She, W. C. L. Lay, R. Wang, A. G. Fane, Coupled effects of internal concentration polarization and fouling on flux behavior of forward osmosis membranes during humic acid filtration, Journal of Membrane Science, 354 (2010) 123–133.

[68] Y. Wang, F. Wicaksana, Ch. Y. Tang, A. G. Fane, Direct microscopic observation of forward osmosis membrane fouling, Environ. Sci. Technol., 44 (2010) 7102–7109.

[69] K. Y. Wang, R. Ch. Ong, T. Chung, Double-Skinned forward osmosis membranes for reducing internal concentration polarization within the porous sublayer, Ind. Eng. Chem. Res, 49 (2010) 4824–4831.

[70] S. Zhang,K. Y. Wang,T. Chung,Y. C. Jean, H. Chen, Molecular design of the cellulose ester-based forward osmosis membranes for desalination, Chemical Engineering Science, 66 (2011) 2008−2018.

[71] R. Chin Ong, T. Chung, B. J. Helmer, and J. S. deWit, Novel Cellulose Esters for Forward Osmosis Membranes, Industrial Engineering Chemistry Research, 51 (2012) 16135−16145.
[72] J. E. Cadotte, R. J. Petersen, R. E. Larson, E. E. Erickson, New thin-film composite seawater reverse-osmosis membrane, Desalination, 32 (1980) 25–31.
[73] S. Loeb, L. Titelman, E. Korngold, J. Freiman, Effect of porous support fabric on osmosis through a Loeb-Sourirajan type asymmetric membrane, J. Membr. Sci., 129 (1997) 243.
[74] R. Wang, L. Shi, Ch. Y. Tang, Sh. Chou. Ch. Qiu, A. G. Fane, Characterization of novel forward osmosis hollow fiber membranes, Journal of Membrane Science, 355 (2010) 158–167.
[75] S. Chou, L. Shi, R. Wang, C. Y. Tang, C. Qiu, A. G. Fane, Characteristics and potential applications of a novel forward osmosis hollow fiber membrane, Desalination, 261 (2010) 365–372.

[76] G. Han, Z. L. Cheng, T. Chung, Thin-film composite (TFC) hollow fiber membrane with double-polyamide active layers for internal concentration polarization and fouling mitigation in osmotic processes, Journal of Membrane Science, 523 (2017) 497–504.

[77] HTI starts producing thin-film composite FO membrane, Membrane Technology 7, 5-6, 2012.

[78] R. Ravanur, I. Roh, J.E. Klare, A. Noy, O. Bakajin, S. Leandro, Thin film composite membranes for forward osmosis, and their preparation methods, United States Patent : US20120080378A1, 2012.

[79] AquaporinInside™ Forward Osmosis (FO) membrane.https://aquaporin.dk/products/fo/

[80] X. Li, Ch. H. Loh, R. Wang, W. Widjajanti, J. Torres, Fabrication of a robust high-performance FO membrane by optimizing substrate structure and incorporating aquaporin into selective layer, Journal of Membrane Science, 525 (2017) 257–268.

[81] R. Malaisamy, A. Talla-Nwafo, K. Berly, L. Jones, Polyelectrolyte modification of nanofiltration membrane for selective removal of monovalent anions, Separation and Purification Technology, 77 (2011) 367–374.

[82] G. Zhang, H. Yan, Sh. Ji, Z. Liu, Self-assembly of polyelectrolyte multilayer pervaporation membranes by a dynamic layer-by-layer technique on a hydrolyzed polyacrylonitrile ultrafiltration membrane, Journal of Membrane Science, 292 (2007) 1–8.

[83] L. Setiawan, R. Wang, K. Li, A. Fane, Fabrication of novel poly(amide–imide) forward osmosis hollow fiber membranes with a positively charged nanofiltration-like selective layer, Journal of Membrane Science, 369 (2011) 196–205.

[84] L. Setiawan, R. Wang, K. Li, G. Fane, Fabrication and characterization of forward osmosis hollow fiber membranes with antifouling NF-like selective layer, Journal of Membrane Science, 394–395 (2012) 80–88.

[85] L. Setiawan, R. Wang, S. Tan, L. Shi, A. G. Fane, Fabrication of poly(amide-imide)-polyethersulfone dual layer hollow fiber membranes applied in forward osmosis by combined polyelectrolyte cross-linking and depositions, Desalination, 312 (2013) 99–106.

[86] Ch. Qiu, L. Setiawan, R. Wang, Ch. Y. Tang, A. G. Fane, High performance flat sheet forward osmosis membrane with an NF-like selective layer on a woven fabric embedded substrate, Desalination, 287 (2012) 266–270.

[87] Q. Saren, Ch. Q. Qiu, Ch. Y. Tang, Synthesis and characterization of novel forward osmosis membranes based on layer-by-layer assembly, Environ. Sci. Technol, 45 (2011) 5201–5208.

[88] C. Liu, X. Lei, L. Wang, J. Jia, X. Liang,X. Zhao, H. Zhu, Investigation on the removal performances of heavy metal ions with the layer-by-layer assembled forward osmosis membranes, Chemical Engineering Journal, 327 (2017) 60-70.

[89] F. Wang, J. Feng, Ch. Gao, Manipulating the properties of coacervated polyelectrolyte microcapsules by chemical crosslinking, Colloid Polym Sci, 286 (2008) 951–957.

[90] S. Wang, J. Cai, W. Ding, Z. Xu, Z. Wang, Bio-inspired aquaporinZ containing double-skinned forward osmosis membrane synthesized through layer-by-layer assembly, Membranes, 5 (2015) 369–384.

[91] X. Liu, H.Y. Ng, Fabrication of layered silica-polysulfone mixed matrix substrate membrane for enhancing performance of thin-film composite forward osmosis membrane, J. Membr. Sci. 481 (2015) 148–163.

[92] J. J. Beh, E. P. Ng, J. Y. Sum, B. S, Ooi, Thermodynamics and kinetics control of support layer synthesis for enhanced thin film composite membrane performance, J. Appl. Polym. Sci, 135 (2017) 45802.

[93] M. Mulder, III /Membrane preparation/ Phase inversion membranes, University of Twente, Enschede, Academic Press, 2000. http://index-of.co.uk/Tutorials 2/MEMBRANE%20PREPARATION%20-%20Phase%20Inversion%20Membranes.pdf.

[94] H. A. Tsai, C. Y. Kuo, J. H. Lin, D. M. Wang, A. Deratani, C. Pochat-Bohatier, K. R. Lee, J. Y. Lai, Morphology control of polysulfone hollow fiber membranes via water vapor induced phase separation, Journal of Membrane Science, 278 (2006) 390–400.

[95] Y. Cai, J. Li, Y. Guo, Z. Cui, Y. Zhang, In-situ monitoring of asymmetric poly(ethylene-co-vinyl alcohol) membrane formation via a phase inversion process by an ultrasonic through-transmission technique, Desalination, 283: 25–30.

[96] B. S. Lalia, V. Kochkodan, R. Hashaikeh, N. Hilal, A review on membrane fabrication: Structure, properties and performance relationship, Desalination, 326 (2013) 77–95.

[97] F. Fu, S. Zhang, Sh. Sun, K. Wang, T. Chung, POSS-containing delamination-free dual-layer hollow fiber membranes for forward osmosis and osmotic power generation, Journal of Membrane Science, 443 (2013) 144–155.

[98] P. Hajighahremanzadeh, M. Abbaszadeh, S. A. Mousavi, M. Soltanieh, H. Bakhshi, Polyamide/polyacrylonitrile thin film composites as forward osmosis membranes, Journal of Applied Polymer Science, 133 (2016) 42.

[99] H. Wu, B. Tang, P. Wu, Development of novel SiO_2–GO nanohybrid/polysulfone membrane with enhanced performance, Journal of Membrane Science, 451 (2014) 94–102.

[100] Ch. Boo, S. Lee, M. Elimelech, Z. Meng, S. Hong, Colloidal fouling in forward osmosis: Role of reverse salt diffusion, Journal of Membrane Science, 390–391 (2012) 277–284.

[101] M. Mulder, Basic Principles of Membrane Technology, Kluwer Academic Publisher, Netherlands, 2e édition, ISBN 0, 8247 (1996) 75.

[102] X. Lu, L. H. A. Chavez, S. R. Castrillo, J. Ma, M. Elimelech, Influence of active layer and support layer surface structures on organic fouling propensity of thin-film composite forward osmosis membranes, Environ. Sci. Technol., 49 (2015) 1436–1444.

[103] X. Li, C. H. Loh, R. Wang, W. Widjajanti, J. Torres, Fabrication of a robust high-performance FO membrane by optimizing substrate structure and incorporating aquaporin into selective layer, Journal of Membrane Science, 525 (2017) 257-268.

[104] E. Fontananova, J. C. Jansen, A. Cristiano, E. Curcio, E. Drioli, Effect of additives in the casting solution on the formation of PVDF membranes, Desalination, 192 (2006) 190–197.

[105] H. Liang, W. Hung, H. Yu, Ch. Hu, K. Lee, J. Lai, Z. Xu, Forward osmosis membranes with unprecedented water flux, Journal of Membrane Science, 529 (2017) 47–54.
[106] H. Liang, K. Ji, L. Zha, W. Hu, Y. Ou, Z. Xu, Polymer membranes with vertically oriented pores constructed by 2D freezing at ambient temperature, ACS Appl. Mater. Interfaces, 8 (2016) 14174–14181.

[107] W. Fang, R. Wang, Sh. Chou, L. Setiawan, A. G. Fane, Composite forward osmosis hollow fiber membranes: Integration of RO- and NF-like selective layers to enhance membrane properties of anti-scaling and anti-internal concentration polarization, Journal of Membrane Science, 394–395 (2012) 140–150.

[108] S. Kaur, D. Rana, T. Matsuura, S. Sundarrajan, S. Ramakrishna, Preparation and characterization of surface modified electrospun membranes for higher filtration flux, Journal of Membrane Science, 390–391 (2012) 235–242.

[109] X. Song, Z. Liu, D. D. Sun, Nano Gives the Answer: Breaking the bottleneck of internal concentration polarization with a nanofiber composite forward osmosis membrane for a high water production rate, Adv. Mater, 23 (2011) 3256–3260.

[110] N. Bui, M. L. Lind, E. M. V. Hoek, J. R. McCutcheon, Electrospun nanofiber supported thin film composite membranes for engineered osmosis, Journal of Membrane Science, 385–386 (2011) 10–19.

[111] M. Tian, R. Wang, K. Goh, Y. Liao, A. G. Fane, Synthesis and characterization of high-performance novel thin film nanocomposite PRO membranes with tiered nanofiber support reinforced by functionalized carbonnanotubes, Journal of Membrane Science, 486 (2015) 151–160.

[112] F. E Ahmed, B. S. Lalia, R. Hashaikeh, A review on electrospinning for membrane fabrication: Challenges and applications, Desalination, 356 (2015) 15–30.

[113] N. Bui, J. R. McCutcheon, Hydrophilic nanofibers as new supports for thin film composite membranes for engineered osmosis, Environ. Sci. Technol., 47 (2013) 1761–1769.

[114] N. Bui, J. R. McCutcheon, Nanoparticle-embedded nanofibers in highly permselective thin-film nanocomposite membranes for forward osmosis, Journal of Membrane Science, 518 (2016) 338–346.

[115] M. R. Chowdhury, L. Huang, J. R. McCutcheon, Thin film composite membranes for forward osmosis supported by commercial nanofiber nonwovens, Ind. Eng. Chem. Res., 56 (2017) 1057–1063.

[116] M. Rastgar, A. Shakeri, A. Bozorg, H. Salehi, V. Saadattalab, Impact of nanoparticles surface characteristics on pore structure and performance of forward osmosis membranes, Desalination, (2017).

[117] G. Z. Ramon, M. C. Wong, E. M. V. Hoek, Transport through composite membrane, part 1: Is there an optimal support membrane?, Journal of Membrane Science, 415–416 (2012) 298–305.

[118] G. Z. Ramon, E. M. V. Hoek, Transport through composite membranes, part2: Impacts of roughness on permeability and fouling, Journal of Membrane Science, 425–426 (2013) 141–148.

[119] D. L. Shaffer, H. Jaramillo, S. R. Castrillon. X. Lu, M. Elimelech, Post-fabrication modification of forward osmosis membranes with a poly (ethyleneglycol) block copolymer for improved organic fouling resistance, Journal of Membrane Science, 490 (2015) 209–219.

[120] S. S. Manickam, J. R. MucCutcheon, Understanding mass transfer through asymmetric membranes during forward osmosis: A historical perspective and critical review on measuring structural parameter with semi-empirical models and characterization approaches, Desalination, 421 (2017) 110–126.

[121] H. I. Kim, S. S. Kim, Plasma treatment of polypropylene and polysulfone supports for thin film composite reverse osmosis membrane, Journal of Membrane Science, 286 (2006) 193–201.

[122] N. Akther, A. Sodiq, A. Giwa, S. Daer, H. A. Arafat, S. W. Hasan, Recent advancements in forward osmosis desalination: A review, Chemical Engineering Journal, 281 (2015) 502–522.

[123] L. A. Hoover, J. D. Schiffman, M. Elimelech, Nanofibers in thin-film composite membrane support layers: Enabling expanded application of forward and pressure retarded osmosis, Desalination, 308 (2013) 73–81.

[124] M. Tian, Ch. Qiu, Y. Liao, Sh. Chou, R. Wang, Preparation of polyamide thin film composite forward osmosis membranes using electrospun polyvinylidene fluoride (PVDF) nanofibers as substrates, Separation and Purification Technology, 118 (2013) 727–736.

[125] S. Lee, Ch. Boo, M. Elimelech, S. Hong, Comparison of fouling behavior in forward osmosis (FO) and reverse osmosis (RO), Journal of Membrane Science, 365 (2010) 34–39.

[126] J. Wei, Ch. Qiu, Ch. Y. Tang, R. Wang, A. G. Fane, Synthesis and characterization of flat-sheet thin film composite forward osmosis membranes, Journal of Membrane Science, 372 (2011) 292–302.

[127] T. Chung, X. Li, R. Ch. Ong, Q. Ge, H. Wang, G. Han, Emerging forward osmosis (FO) technologies and challenges ahead for clean water and clean energy applications, Current Opinion in Chemical Engineering, 1 (2012) 246–257.

[128] H. R. Ahn, T. M. Tak, Y. N. Kwon, Preparation and applications of poly vinyl alcohol (PVA) modified cellulose acetate (CA) membranes for forward osmosis (FO) processes, Desalin. Water Treat, 53 (2015) 1–7.

[129] M. F. Flanagan, I. C. Escobar, Novel charged and hydrophilizedpolybenzimidazole (PBI) membranes for forward osmosis, Journal of Membrane Science, 434 (2013) 85–92.

[130] Q. Wang, Y. B. Zhao, H. B. Xu, Y. J. Yang, Thermo sensitive phase transitions kinetics of poly(N-isopropylacrylamide-co-acrylamide) microgelaqueous dispersions, J. Appl. Polym. Sci, 113 (2009) 321–326.

[131] A. Saraf, K, Johnson, M. L. Lind, Poly(vinyl) alcohol coating of the support layer of reverse osmosis membranes to enhance performance in forward osmosis, Desalination, 333 (2014) 1–9.

[132] L. Zhang, Q. She, R. Wang, S. Wongchitphimon, Yunfeng Chen, Anthony G. Fane, Unique roles of aminosilane in developing anti-fouling thin film composite (TFC) membranes for pressure retarded osmosis (PRO), Desalination, 389 (2016) 119–128.

[133] Y. Li, T. Chung, Highly selective sulfonated polyethersulfone (SPES)-based membranes with transition metal counterions for hydrogen recovery and natural gas separation, Journal of Membrane Science, 308 (2008) 128–135.

[134] Sh. Chen, K. Yu, Sh. Lin, D. Chang, R. M. Liou, Pervaporation separation of water/ethanol mixture by sulfonated polysulfone membrane, Journal of Membrane Science, 183 (2001) 29–36.

[135] X. Liu, S. L. Ong, H. Y. Ng, Fabrication of mesh-embedded double-skinned substrate membrane and enhancement of its surface hydrophilicity to improve anti-fouling performance of resultant thin-film composite forward osmosis membrane, Journal of Membrane Science, 511 (2016) 40–53.

[136] K. Y. Wang, T. Chung, G. Amy, Developing thin-film-composite forward osmosis membranes on the PES/SPSf substrate through interfacial polymerization, AIChE Journal, 58 (2012) 3.

[137] Ch. Zhao, J. Xue, F. Ran, Sh. Sun, Modification of polyethersulfone membranes–A review of methods, Progress in Materials Science, 58 (2013) 76–150.

[138] C. Dizman, M. A.Tasdelen, Y. Yagci, Recent advances in the preparation of functionalized polysulfones, Polym Int, 62 (2013) 991–1007.

[139] S. Sahebi, Sh. Phuntsho, Y. Ch. Woo, M. J. Park, L. D. Tijing, S. Hong, H. K. Shon, Effect of sulphonated polyethersulfone substrate for thin film composite forward osmosis membrane, Desalination, 389 (2016) 129–136.

[140] Y. Wang, T. Xu, Anchoring hydrophilic polymer in substrate: An easy approach for improving the performance of TFC FO membrane, Journal of Membrane Science, 476 (2015) 330–339.

[141] A. Noshay, L. M. Robeson, Sulfonated polysulfone, Journal of Applied Polymer Science, 20 (1976) 1885–1903.

[142] M. Hung, S. Chen, R. Liou, Ch. Hsu, J. Lai, W. E. Mickols, Contacting with ammonia or alkylamine: U.S. Patent 5,755,964 [P]. 1998-5-26, in. Journal of Applied Polymer Science, 90 (2003) 3374–3383.

[143] N. Widjojo, T. Chung, M. Weber, Ch. Maletzkoc, V. Warzelhanb, The role of sulphonated polymer and macrovoid-free structure in the support layer for thin-film composite (TFC) forward osmosis (FO) membranes, Journal of Membrane Science, 383 (2011) 214–223.

[144] N. Widjojo, T. Chung, M. Weber, Ch. Maletzko, V. Warzelhan, A sulfonated polyphenylenesulfone (sPPSU) as the supporting substrate in thin film composite (TFC) membranes with enhanced performance for forward osmosis (FO), Chemical Engineering Journal, 220 (2013) 15–23.

[145] P. Zhong, X. Fu, T. Chung, M. Weber, Ch. Maletzko, Development of thin-film composite forward osmosis hollow fiber membranes using direct sulfonated polyphenylenesulfone (sPPSU) as membrane substrates, Environ. Sci. Technol, 47 (2013) 7430–7436.

[146] H. B. Park, B. D. Freeman, Z. Zhang, M. Sankir, J. E. McGrath, Highly chlorine-tolerant polymers for desalination, Angew. Chem, 120 (2008) 6108–6113.

[147] D. MoÈckel, E. Staude, M. D. Guiver, Static protein adsorption, ultrafiltration behavior and cleanability of hydrophilized polysulfone membranes, Journal of Membrane Science, 158 (1999) 63–75.

[148] X. Zhang, J. Tian, Z. Ren, W. Shi, Z. B. Zhang, Y. P. Xu, Sh. Sh. Gao, F. Cui, High performance thin-film composite (TFC) forward osmosis (FO) membrane fabricated on novel hydrophilic disulfonated poly (arylene ether sulfone) multi block copolymer/polysulfone substrate, Journal of Membrane Science, 520 (2016) 529–539.

[149] Y. H. Cho, J. Han, S. Han, M. D. Guiver, H. B. Park, Polyamide thin-film composite membranes based on carboxylated polysulfone microporous support membranes for forward osmosis, Journal of Membrane Science, 445 (2013) 220–227.

[150] D. Wang, W. Zou, L. Li, Q. Wei, Sh. Sun, Ch. Zhao, Preparation and characterization of functional carboxylic polyethersulfone membrane, Journal of Membrane Science, 374 (2011) 93–101.

[151] W. L. Harrison, M. A. Hickner, Y. S. Kim, J. E. McGrath, Poly(aryleneether sulfone) copolymers and related systems from disulfonated monomer building blocks: synthesis, characterization, and performance—a topical review, Fuel Cells, 5 (2005) 201–212.

[152] P. H. H. Duong, S. Chisca, P. Hong, H. Cheng, S. P. Nunes, T. Chung, Hydroxyl functionalized polytriazole-co-polyoxadiazole as substrates for forward osmosis membranes, Appl. Mater. Interfaces, 7 (2015) 3960–3973.

[153] D. Gomes, J. Roeder, M. L. Ponce, S. P. Nunes, Characterization of partially sulfonated polyoxadiazoles and oxadiazole–triazole copolymers, Journal of Membrane Science, 295 (2007) 121–129.

[154] Y. Tang, N. Widjojo, G. M. Shi, T. Chung, M. Weber, Ch. Maletzko, Development of flat-sheet membranes for C1–C4 alcohols dehydration via pervaporation from sulfonated polyphenylsulfone (sPPSU), Journal of Membrane Science, 415–416 (2012) 686–695.

[155] L. Chen, Ch. Wu, M. Chen, K. Hsu, H. Li, Ch. Hsieh, M. Hsiao, Ch. Chang, P. P. Chu, Cross-linked norbornene sulfonated poly(ether ketone)s for proton exchange membrane, Journal of Membrane Science, 361 (2010) 143–153.

[156] P. P. Chu, C. S. Wu, P. C. Liu, T. H. Wang, J. P. Pan, Proton exchangemembrane bearing entangled structure: sulfonated poly(ether etherketone)/bismaleiminde hyperbranch, Polymer, 51 (2010) 1386–1394.

[157] G. Han, T. Chung, M. Toriida, Sh. Tamai, Thin-film composite forward osmosis membranes with novel hydrophilic supports for desalination, Journal of Membrane Science, 423–424 (2012) 543–555.

[158] X. Zhang, L. Shen, W. Lang, Y. Wang, Improved performance of thin-film composite membrane with PVDF/PFSA substrate for forward osmosis process, Journal of Membrane Science, 535 (2017) 188–199.

[159] H. Zuo, H. Lu, G. Cao, M. Wang, Y. Wang, J. Liu, Ion exchange resin blended membrane: Enhanced water transfer and retained salt rejection for forward osmosis, Desalination, 421 (2017) 12–22.

[160] B. Jeong, E. M. V. Hoek, Y. Yan, A. Subramani, X. Huang, G. Hurwitz, A. K. Ghosh, A. Jawor, Interfacial polymerization of thin film nanocomposites: A new concept for reverse osmosis membranes, Journal of Membrane Science, 294 (2007) 1–7.

[161] T. Chung, L. Y. Jiang, Y. Li, S. Kulprathipanj, Mixed matrix membranes (MMMs) comprising organic polymers with dispersed inorganic fillers for gas separation, Prog. Polym. Sci, 32 (2007) 483–507.

[162] S. H. Strogatz, D. M. Abrams, A. McRobie, B. Eckhardt, E. Ott, Enhanced flow in carbon nanotubes, NATURE, 438 (2005) 3.

[163] H. Zhao, L. Wu, Z. Zhou, L. Zhang, H. Chen, Improving the antifouling property of polysulfone ultrafiltration membrane by incorporation of isocyanate-treated graphene oxide, Phys. Chem. Chem. Phys, 15 (2013) 9084.

[164] Y. Wang, R. Ou, H. Wang, T. Xu, Graphene oxide modified graphitic carbon nitride as a modifier for thin film composite forward osmosis membrane, Journal of Membrane Science, 475 (2015) 281–289.

[165] S. Morales-Torres, C.M. P. Esteves, J. Figueiredo, Adrián M. T. Silva, Thin-film composite forward osmosis membranes based on polysulfone supports blended with nano structured carbon materials, Journal of Membrane Science, 520 (2016) 326–336.

[166] Z. Low, Q. Liu, E. Shamsaei, X. Zhang, H. Wang, Preparation and characterization of thin-film composite membrane with nanowire-modified support for forward osmosis process, Membranes, 5 (2015) 136-149.

[167] S. H. Kim, S. Kwak, B. Sohn, T. H. Park, Design of TiO_2 nanoparticle self-assembled aromatic polyamide thin-film-composite (TFC) membrane as an approach to solve biofouling problem, Journal of Membrane Science, 211 (2003) 157–165.

[168] W. Kuang, Z. Liu, G. Kang, D. Liu, M. Zhou, Y. Cao, Thin film composite forward osmosis membranes with poly(2-hydroxyethyl methacrylate) grafted nano-TiO_2 as additive in substrate, J. APPL. POLYM. SCI, (2016).

[169] L. Y. Ng, A. Mohammad, Ch. P. L. N. Hilal, Polymeric membranes incorporated with metal/metal oxide nanoparticles: A comprehensive review, Desalination, 308 (2013) 15–33.

[170] W. Kuang, Z. Liu, H. Yu, G. Kang, X. Jie, Y. Jin, Y. Cao, Investigation of internal concentration polarization reduction in forward osmosis membrane using nano-$CaCO_3$ particles as sacrificial component, Journal of Membrane Science, 497 (2016) 485–493.

[171] P. Lu, Sh. Liang, L. Qiu, Y. Gao, Q. Wang, Thin film nanocomposite forward osmosis membranes based on layered double hydroxide nanoparticles blended substrates, Journal of Membrane Science, 504 (2016) 196–205.

[172] M. Obaid, Z. Kh. Ghouri, O. A. Fadali, Kh. A. Khalil, A. A. Almajid, N. A. M. Barakat, Amorphous SiO_2 NP-incorporated poly(vinylidene fluoride) electrospun nanofiber membrane for high flux forward osmosis desalination, ACS Appl. Mater. Interfaces, 8 (2016) 4561–4574.

[173] G. Kang, Y. Cao, Application and modification of poly(vinylidene fluoride) (PVDF) membranes – A review, Journal of Membrane Science, 463 (2014) 145–165.

[174] X. Lu, S. V. Castrillon, D. L. Shaffer, J. Ma, M. Elimelech, In situ surface chemical modification of thin-film composite forward osmosis membranes for enhanced organic fouling resistance, Environ. Sci. Technol,47 (2013) 12219–12228.

[175] S. R. Castrillón, X. Lu, D. L. Shaffer, M. Elimelech, Amine enrichment and poly(ethyleneglycol)(PEG) surface modification of thin-film composite forward osmosis membranes for organic fouling control, Journal of Membrane Science, 450 (2014) 331–339.

[176] A. Nguyen, L. Zou, C. Pries, Evaluating the antifouling effects of silver nanoparticles regenerated by TiO_2 on forward osmosis membrane, Journal of Membrane Science, 454 (2014) 264–271.

[177] Y. Gao, M. Hu, B. Mi, Membrane surface modification withTiO_2–graphene oxide for enhanced photocatalytic performance, Journal of Membrane Science, 455 (2014) 349–356.

[178] Ch. D. Vecitis, M. H. Schnoor, M. S. Rahaman, J. D. Schiffman, M. Elimelech, Electrochemical multiwalled carbon nanotube filter for viral and bacterial removal and inactivation, Environ. Sci. Technol, 45 (2011) 3672–3679.

[179] R. W. Holloway, A. E. Childress, K. E. Dennett, T. Y. Cath, Forward osmosis for concentration of anaerobic digester centrate, Water Research, 41 (2007) 4005–4014.

[180] K. Zodrow, L. Brunet, Sh. Mahendra, D. Li, A. Zhang, Q. Li, P. J. J. Alvarez, Polysulfone ultrafiltration membranes impregnated with silver nanoparticles show improved biofouling resistance and virus removal, Water Research, 43 (2009) 715–723.

[181] J. Yin, Y. Yang, Z. Hu, B. Deng, Attachment of silver nanoparticles (Ag NPs) on to thin-film composite (TFC) membranes through covalent bonding to reduce membrane biofouling, Journal of Membrane Science, 441 (2013) 73–82.

[182] A. Adout, S. Kang, A. Asatekin, A. M. Mayes, M. Elimelech, Ultrafiltration membranes incorporating amphiphilic comb copolymer additives prevent irreversible adhesion of bacteria, Environ. Sci. Technol, 44 (2010) 2406–2411.

[183] S. Kang, A. Asatekin, A. M. Mayes, M. Elimelech, Protein antifouling mechanisms of PAN UF membranes incorporating PAN-g-PEO additive, Journal of Membrane Science, 296 (2007) 42–50.

[184] A. C. Sagle, E. M. Van Wagner, H. Jua, B. D. McCloskey, B. D. Freeman, M. M. Sharma, PEG-coated reverse osmosis membranes: Desalination properties and fouling resistance, Journal of Membrane Science, 340 (2009) 92–108.

[185] J. Mansouri, S. Harrisson, V. Chen, Strategies for controlling biofouling in membrane filtration systems: Challenges and opportunities, J. Mater. Chem, 20 (2010) 4567–4586.

[186] N. D. Brault, Ch. Gao, H. Xue, M. Piliarik, J. Homola, Sh. Jiang, Q. Yua, Ultra-low fouling and functionalizable zwitterionic coatings grafted onto SiO_2 via a biomimetic adhesive group for sensing and detection in complex media, Biosensors and Bioelectronics, 25 (2010) 2276–2282.

[187] S. Azari, L. Zou, Using zwitterionic amino acid l-DOPA to modify the surface of thin film composite polyamide reverse osmosis membranes to increase their fouling resistance, Journal of Membrane Science, 401–402 (2012) 68–75.

[188] R. Hausman, B. Digman, I. C. Escobar, M. Coleman, T. Chung, Functionalization of polybenzimidizole membranes to impart negative charge and hydrophilicity, Journal of Membrane Science, 363 (2010) 195–203.

[189] J. T. Arena, S. S Manickam, K. K. Reimund, B. D. Freeman, J. R. McCutcheon Solute and water transport in forward osmosis using polydopamine modified thin film composite membranes, Desalination, 343 (2014) 8–16.

[190] H. Lee, S. M. Dellatore, W. M. Miller, P. B. Messersmith, Mussel-inspired surface chemistry for multifunctional coatings, Science, 318 (2007) 426–430.

[191] Q. Ye, F. Zhou, W. M. Liu, Bioinspired catecholic chemistry for surface modification, Chem. Soc. Rev., 40 (2011) 4244–4258.

[192] J. T. Arena, B. McCloskey, B. D. Freeman, J. R. McCutcheon, Surface modification of thin film composite membrane support layers with polydopamine: enabling use of reverse osmosis membranes in pressure retarded osmosis, Journal of Membrane Science, 375 (2011) 55–62.

[194] G. Han, S. Zhang, X. Li, N. Widjojo, T. Chung, Thin film composite forward osmosis membranes based on polydopamine modified polysulfone substrates with enhancements in both water flux and salt rejection, Chemical Engineering Science, 80 (2012) 219–231.

[195] F. Peng, X. Huang, A. Jawor, E. M. V. Hoek, Transport, structural, and interfacial properties of poly (vinyl alcohol)–polysulfone composite nanofiltration membranes, Journal of Membrane Science, 353 (2010) 169–176.

[196] S. Kim, K. Lee, Poly (vinyl alcohol) membranes having an integrally skinned asymmetric structure, Mol. Cryst. Liq. Cryst, 512 (2009) 32.

[197] Y. Zhang, H. Li, H. Li, R. Li, C. Xiao, Preparation and characterization of modified polyvinyl alcohol ultrafiltration membranes, Desalination, 192 (2006) 214–223.

[198] H. A. Shawky, Synthesis of ion-imprinting Chitosan/PVA crosslinked membrane for selective removal of Ag(I), Journal of Applied Polymer Science, 114 (2009) 2608–2615.

[199] A. L. Ahmad, N. M. Yusuf, B. S. Ooi, Preparation and modification of poly (vinyl) alcohol membrane: Effect of crosslinking time towards its morphology, Desalination, 287 (2012) 35–40.

[200] Q. Liu, J. Li, Z. Z. Zhou, J. Xie, J. Y. Lee, Hydrophilic mineral coating of membrane substrate for reducing internal concentration polarization (ICP) in forward osmosis, Nature/Scientific Reports, 6 (2016) 19593.

[201] P. Chen, Z. Xu, Mineral-coated polymer membranes with superhydrophilicity and underwater superoleophobicity for effective oil/water separation, Nature/Scientific reports, 3 (2013) 2776.

[202] S. Zhi, L. Wan, Z. Xu, Poly(vinylidene fluoride)/poly(acrylicacid)/calcium carbonate composite membranes via mineralization, Journal of Membrane Science, 454 (2014) 144–154.

[203] P. Sh. Zhong, T. Chung, K. Jeyaseelan, A. Armugam, Aquaporin-embedded biomimetic membranes for nanofiltration, Journal of Membrane Science, 407–408 (2012) 27–33.

[204] W. Xie, F. He, B. Wang, T. Chung, K. Jeyaseelan, A. Armugam, Y. W. Tong, An aquaporin-based vesicle-embedded polymeric membrane for low energy water filtration, J. Mater. Chem. A, 1 (2013) 7592.

[205] H. L. Wang, T. Chung, Y. W. Tong, K. Jeyaseelan, A. Armugam, H. H. Ph. Duong, F. Fu, H. Seah, J. Yang, M. Hong, Mechanically robust and highly permeable AquaporinZ biomimetic membranes, Journal of Membrane Science, 434 (2013) 130–136.

[206] W. Ding, J. Cai, Z. Yu, Q. Wang, Z. Xu, Z. Wang, C. Gao, Fabrication of an aquaporin-based forward osmosis membrane through covalent bonding of a lipid bilayer to a microporous support, J. Mater. Chem. A, 3 (2015) 20118.

[207] G. T. Gray, J. R. McCutcheon, M. Elimelech, Internal concentration polarization in forward osmosis" role of membrane orientation, Desalination, 197 (2006) 1–8.

[208] Ch. Qiu, S. Qi, Ch. Y. Tang, Synthesis of high flux forward osmosis membranes by chemically crosslinked layer-by-layer polyelectrolytes, Journal of Membrane Science, 381 (2011) 74–80.

[209] P. Sukitpaneenit, T. Chung, High performance thin-film composite forward osmosis hollow fiber membranes with macrovoid-free and highly porous structure for sustainable water production, Environ. Sci. Technol., 469 (2012) 7358−7365.

[210] Y. Gu, Y. Wang, J. Wei, Ch. Y. Tang, Organic fouling of thin-film composite polyamide and cellulose triacetate forward osmosis membranes by oppositely charged macromolecules, Water Research 47 (2013) 1867−1874.

[211] K. Goh, L. Setiawan, L. Wei, W. Jiang, R. Wang, Y. Chen, Fabrication of novel functionalized multi-walled carbon nanotube immobilized hollow fiber membranes for enhanced performance in forward osmosis process, Journal of Membrane Science, 446 (2013) 244–254.

[212] Z. Zhou, J. Y. Lee, T. Chung, Thin film composite forward-osmosis membranes with enhanced internal osmotic pressure for internal concentration polarization reduction, Chemical Engineering Journal, 249 (2014) 236–245.

[213] J. M. Puguan, H. Kim, K. Lee, H. Kim, Low internal concentration polarization in forward osmosis membranes with hydrophilic cross linked PVA nanofibers as porous support layer, Desalination, 336 (2014) 24–31.

[214] N. Niksefat, M. Jahanshahi, A. Rahimpour, The effect of SiO_2 nanoparticles on morphology and performance of thin film composite membranes for forward osmosis application, Desalination, 343 (2014) 140–146.

[215] D. Emadzadeh, W. J. Lau, T. Matsuura, A. F. Ismail, M. Rahbari-Sisakht, Synthesis and characterization of thin film nanocomposite forward osmosis membrane with hydrophilic nanocomposite support to reduce internal concentration polarization, Journal of Membrane Science, 449 (2014) 74–85.

[216] M. Shibuya, M. Yasukawa, T. Takahashi, T. Miyoshi, M. Higa, H. Matsuyama, Effects of operating conditions and membrane structures on the performance of hollow fiber forward osmosis membranes in pressure assisted osmosis, Desalination, 365 (2015) 381–388.

[217] L. Huang, J. R. McCutcheon, Impact of support layer pore size on performance of thin film composite membranes for forward osmosis, Journal of Membrane Science, 483 (2015) 25–33.

[218] Sh. Lin, Mass transfer in forward osmosis with hollow fiber membranes, Journal of Membrane Science, 514 (2016) 176–185.

[219] Z. Dabaghian, A. Rahimpour, M. Jahanshahi, Highly porous cellulosic nanocomposite membranes with enhanced performance for forward osmosis desalination, Desalination, 381 (2016) 117–125.

[220] E. Tian, X. Wang, Y. Zhao, Y. Ren, Middle support layer formation and structure in relation to performance of three-tier thin film composite forward osmosis membrane, Desalination, (2017).

[221] M. Yasukawa, Sh. Mishima, Y. Tanaka, T. Takahashi, H. Matsuyama, Thin-film composite forward osmosis membrane with high water flux and high pressure resistance using a thicker void-free polyketone porous support, Desalination, 402 (2017) 1–9.

[222] X. Chen, J. Xu, J. Lu, B. Shan, C. Gao, Enhanced performance of cellulose triacetate membranes using binary mixed additives for forward osmosis desalination, Desalination, 405 (2017) 68–75.